T. R.
BOLU ABANT IZZET BAYSAL UNIVERSITY
INSTITUTE OF GRADUATE STUDIES
Department of Mechanical Engineering

ENTROPY GENERATION MINIMIZATION FOR DIFFERENT TYPES OF HEAT EXCHANGERS USING NANOFLUIDS

MASTER OF SCIENCE

MUSAAB ABDULRAHMAN HUWAISH

ACADEMIC SUPERVISOR
Prof. Dr./Assist. Kadir GELIS

BOLU, JANUARY - 2023

APPROVAL OF THE THESIS

ENTROPY GENERATION MINIMIZATION FOR DIFFERENT TYPES OF HEAT EXCHANGERS USING NANOFLUIDS submitted by **MUSAAB ABDULRAHMAN HUWAISH** and defended before the Examining Committe Members listed below in partial fulfi ment of the requirements for the degree of **Master of Science** in **Department of Mechanıcal Engineering, Institute of Graduate Studies of Bolu Abant Izzet Baysal University in 6.01.2023** by

Examining Committee Members	**Signature**
Supervisor Prof. Dr./Assist. Kadir GELİŞ Bolu Abant Izzet Baysal University	....
Member Prof. Dr./ Assoc. Eda Feyza AKYÜREK Erzurum Technical University	....
Member Prof. Dr./ Assoc Alaattin Osman EMİROĞLU Bolu Abant Izzet Baysal University	....

Prof. Dr. İbrahim KÜRTÜL
Director of Instıtute of Graduate Studies

ETHICAL DECLARATION

In this thesis dissertation that was properly prepared according to the Thesis Writing Rules of Bolu Abant İzzet Baysal University of the Institute of Graduates Studies, I hereby declare that.

- All data, information, and documents presented in the thesis were obtained in accordance with the academic and ethical rules,
- All data, documents, assessments, and results were presented in accordance with the scientific ethical and moral rules,
- All works that were benefitted in the thesis were appropriately cited,
- No alteration was made in the data used,
- Study presented in this thesis is original,

Otherwise, I declare that I accept the loss of all my rights in case any contradiction that may arise against me.

Based on the plagiarism report that was generated on the date of 29/12/2022 by using predetermined filtrations set by Directorate of Institute of Graduate Studies of the Turnitin programme, a plagiarism\detection sofware, the similarity index detected was 22 %.

____

Musaab Abdulrahman HUWAISH

ABSTRACT

ENTROPY GENERATION MINIMIZATION FOR DIFFERENT TYPES OF HEAT EXCHANGERS USING NANOFLUIDS
MSC THESIS
MUSAAB ABDULRAHMAN HUWAISH
BOLU ABANT IZZET BAYSAL UNIVERSITY
INSTITUTE OF GRADUATE STUDIES
DEPARTMENT OF MECHANICAL ENGINEERING
(SUPERVISOR: PROF. DR./ASSIST. KADİR GELIS)

BOLU, JANUARY 2023
xiii + 69

In recent years, many engineers and researchers have tried to improve the thermal performance of heat exchangers. Heat exchanger efficiency may be improved using a variety of technologies. For decades, efforts have been made by researchers to increase heat transfer in heat exchangers, shorten the time it takes for heat to exchange, and improve system performance. Despite the importance of fins in increasing heat transfer, they make the heat exchanger of great weight and size, which is one of its disadvantages. Changes in flow shape, boundary conditions, or the fluid's thermal conductivity can all help posativily improve heat transfer by convection. Many strategies have been proposed to enhance the fluids' ability to transmit heat. The usage of nanofluilds are one of the strategies. Nanofluids have different heat transfer potentials in different applications. This study used different volume concentrations (%wt 0.1-0.2-0.3) of SiO_2/Water nanofluids with shell and tube, plate, and double-pipe heat exchangers to improve their performance and reduce entropy generation. For each heat exchanger, heat transfer and entropy generation minimization calculations were made within the scope of experimental parameters. In the study, the total heat transfer coefficient, efficiency, number of transfer units and entropy production were calculated. Response Surface Method (RSM) was used to determine the effect levels of the parameters. The results are compared to water when the SiO_2/Water nanofluid is used; it has been shown that entropy can be reduced by 56.50% for the plate heat exchanger, 51.70% for the shell and tube heat exchanger, and 39.32% for the concentric heat exchanger.

KEYWORDS: Entropy Generation, Ɛ-NTU, Heat Exchangers, Nanofluids, Response Surface Methodology, RSM

ÖZET

NANOAKIŞKANLAR KULLANARAK FARKLI TİP ISI DEĞİŞTİRİCİLERİ İÇİN ENTROPİ ÜRETİMİNİN MİNİMİZASYONU
YÜKSEK LİSANS TEZİ
MUSAAB ABDURAHMAN HUWAISH
BOLU ABANT İZZET BAYSAL ÜNİVERSİTESİ
LİSANSÜSTÜ EĞİTİM ENSTİTÜSÜ
MAKİNE MÜHENDİSLİĞİ BÖLÜMÜ

(TEZ DANIŞMANI: DR. ÖĞR. ÜYESİ KADİR GELIS)
BOLU, OCAK - 2023
xiii + 69

Son yıllarda birçok mühendis ve araştırmacı ısı değiştiricilerin termal performansını iyileştirmeye çalışmışlardır. Isı değiştiricilerin verimlilikleri çeşitli teknolojiler kullanılarak iyileştirilebilir. Araştırmacılar son yıllarda, ısı değiştiricilerin performansını arttırmak, ısı alışverişi için gereken süreyi kısaltmak ve sistem performansını iyileştirmek için çaba göstermişlerdir. Kanatçıkların ısı değiştiricilerin ısı transferini arttırmasına rağmen, ağırlık ve boyuttaki artışa neden olmaları dezavantajlarından biridir. Akış şekli, sınır koşulları veya sıvının termal iletkenliğindeki değişikliklerin tümü, konveksiyon yoluyla ısı transferini pozitif olarak iyileştirmeye yardımcı olabilir. Sıvıların ısı iletim performanslarını geliştirmek için birçok strateji önerilmiştir. Nanoakışkan kullanımı bu stratejilerden bir tanesidir. Nanoakışkanlar, farklı uygulamalarda farklı ısı transfer potansiyellerine sahiptir. Bu çalışma, gövde borulu, plakalı ve eş merkezli ısı değiştiricileri performanslarını artırmak ve entropi oluşumunu azaltmak için, farklı hacim konsantrasyonlarında (%wt 0.1-0.2-0.3) SiO_2 /Su nanoakışkanları kullanmıştır. Her bir ısı değiştiricisi için deneysel parametreler kapsamında ısı transferi ve entropi üretimi minimizasyonu hesabı yapılmıştır. Çalışmada toplam ısı transfer katsayısı, etkenlik, birim transfer katsayısı ve entropi üretiimi hesaplanmıştır. Parametrelerin etki seviyelerini belirlemek için Yanıt Yüzey Yöntemi (YYY) kullanılmıştır. Sonuçlar, SiO_2 /Su nanoakışkanı kullanıldığı durumda suya göre; plakalı ısı değiştirici için %56.50, gövde borulu ısı değiştirici %51.70, eş merkezli ısı değiştirici için %39.32 oranınde entropinin azalabileceğini göstermiştir.

ANAHTAR KELİMELER: Entropi Üretimi, Ɛ-NTU, Isı Değiştiriciler, Nanoakışkanlar, Yanıt Yüzey Yöntemi

TABLE OF CONTENTS

LIST OF FIGURES

Page

LIST OF TABLES

Page

LIST OF PICTURES

Page

LIST OF ABBREVIATIONS AND SYMBOLS

HEX	: Heat Exchanger
PHE	: Plate Heat Exchanger
STHE	: Shell and Tube Heat Exchanger
DPHE	: Double Pipe Heat Exchanger
NTU	: Number of Transfer Units
RSM	: Response Surface Method
CFD	: Computational fluid dynamics
CNT	: Carbon Nanotube
ε	: Effectiveness
μ	: Dynamic viscosity (Pa.s)
ϕ	: Particle volume concentration (%)
ρ	: Density(kg/m^3)
η	: Heat transfer enhancement
A	: Area (m^2)
C_p	: Specific heat capacity (J/kg. K)
$\dot{m}$	: Mass flow rate (kg/s)
$\dot{V}$	: Volumetric flow rate (kg/s)
T	: Temperature (K)
U	: Overall heat transfer (W/m^{2}K)
out	: Outlet
in	: Inlet
nf	: Nanofluid
np	: Nanoparticle
th	: Thermal
bf	: Base fluid
P	: Pressure
ΔP	: Pressure drop
h	: Enthalpy
Nu	: Nusselt number
f	: Friction factor

ACKNOWLEDGEMENTS

I extend my thanks and gratitude to my supervisor, **Dr. Kadir GELIŞ**. He was a professor, teacher, and brother. He did not skimp on providing informations, even for a single moment.

Thanks to all the teaching staff at the Faculty of Engineering, Abant Izzet Baysal University, headed by **Prof. Dr. Ömer ÖZYURT**, Dean of the Faculty and Head of the Department.

The respected teacher, **Kadir ÖZBEK**, had the most significant role in overcoming problems and obstacles. For him, many thanks and gratitude.

Finally, thanks to **my parents**, my **father** and **mother** had the most significant role in getting me to where I am now.

1. INTRODUCTION

One of the most important issues at the present time is the issue of energy conservation, undoubtedly, the most pressing problem in the future will be this issue. Therefore, researchers, and scientists are working hard to address this critical issue. Advances in cooling, and heating in industrial appliances lead to energy savings and improved heat-transmission, as well as an increase in the equipment's operating life. The efficient use of energy can be used to save energy. Some ways to save energy include energy conversion, conservation, and recovery. Heat exchangers are primarily employed in several technical operations, including the chemical, food, and power-generating industries and air conditioning. Due to high energy prices and limited energy supplies, significant attempts are being made to improve heat exchanger efficiency. The convective heat transfer coefficient, which is caused by various thermophysical parameters of the liquid, such as thermal conductivity and viscosity, has a great influence on the effectiveness of heat exchange. The resulting heat transfer coefficient of thermal conductivity and viscosity greatly affect the heat transfer efficiency (1). Heat exchangers are used in various industrial applications (2).

Heat exchanger efficiency may be improved using a variety of technologies. In order to transfer heat in heat exchangers, strenuous efforts have been made to improve system performance and reduce the time spent by the exchanger for heat exchange. The fins are important in heat transfer, but they increase the size and weight of the exchanger, so many researchers have resorted to improving the fluid used to transfer heat in the exchanger. The most effective process is to add some additives with good conductivity to the fluid to improve heat transfer. Nanotechnology has recently provided a solution to this problem. Choi (3) developed the concept of "nanofluid" in 1995 to enhance the heat transfer properties of conventional fluids.

Due to the limited thermal conductivity of liquids like oil, water, and ethylene glycol, high-density heat cannot be transported via conventional methods. The poor thermal conductivity of the above-mentioned typical fluids is the key limiting their heat transmission capabilities. One way to bypass this restriction is to use the power of small particles. Smaller particles have high strength, which helps bypass this restriction (4). When micrometer or nanometer-sized particles are added to a base fluid, their base fluids show distinctive and enhanced features. These improved fluids might be helpful in various industries, including power generation (5), medicines, and environmental processes (6). Over solid/liquid suspensions, the large surface area of the nanofluids increases the heat transfer capacity, and the Brownian motion of the particles leads to increased dispersion, and this is what distinguishes nanofluids from conventional liquids (7). Nanofluid preparation is critical in improving fluid thermal conductivity using nanoparticles. Shape, volume concentration, nanoparticle size, acidity, and material composition are some of the factors that impact the thermal conductivity of nanofluids (8). Using SiO_2 nanoparticles suspended in water, Julia et al. (9) conducted heat transfer tests in the turbulent Reynolds number range of 3000 to 100000. SiO_2 nanoparticles were used in tests by Kulkarni et al. (10) that involved a 60:40% by weight combination of ethylene glycol/water. They investigated the relationship between particle diameter and viscosity in the (%wt 2–10) particle volume concentration range using particles with diameters of 20 nm, 50 nm, and 100 nm. From their experiments, they deduced those heat transfer coefficients rise with particle dimension. The research using SiO_2 nanofluid shows that the heat transfer coefficient improves as particle concentration increases. Several researchers' investigations for particle concentrations up to 19% and bulk temperatures of 70 °C have shown that the nanofluid is stable at high concentrations and temperatures. Particle size does not significantly affect convective heat transfer coefficients, according to earlier studies. Additionally, the largest heat transfer coefficient is seen in the turbulent area of Reynolds numbers (11).

1.1 Literature Review

Increasing energy consumption rates lead to the depletion of crude oil reserves in decades or centuries. Environmental issues such as global warming and sea level rise are unavoidable outcomes of the continued energy consumption trend. Despite worldwide rules aimed at reducing greenhouse gas emissions, air pollution remains a significant contributor to spreading dangerous illnesses (12).

Many years ago, many people sought to increase the efficiency of heat exchange, the time during which heat is transferred, and ultimately increase the efficiency of heat consumption. For instance, one of the most common passive and active methods utilized in these endeavors is to create turbulence (13). Heat exchangers are important in many energy applications, power plants, and automobiles, according to many scientists investigating or reviewing strategies to alleviate this serious issue. Thermal energy is transferred between two or more fluids via HEXs (14). Water circulates as a hot liquid in the tubes, while nanofluids circulate as a coolant in the case. Using the finite element method, numerical experiments were carried out using COMSOL 5.4 CFD software to solve the continuity, momentum, and energy equations. The obtained results showed that higher entry velocity and volume fraction increased heat transfer, with the Nusselt numbers increasing by (%wt 0.1, 3.96, and 7.62) for volumetric concentration (%wt 1, 2, and 3) , respectively, and the friction factor increasing by (%wt 22.41, 24.14, and 26.72) respectively (15). Qi C et al. (16) investigated that the nanoparticle mass fractions (%wt 0.1 - 0.5) and Reynolds numbers (800-10000) on heat transfer capability and nanofluid flow. Rohit S. Khedkar et al. (17) are transferred heat from water to nanofluids of varying concentrations in a concentric tubular heat exchanger Using different volume percentages of nanoparticles in base fluids. The conclusions were contrasted with clear water. Farajollahi B. et al. (18) are Investigated the effects of particle type, volumetric concentration, and Piclite number suspended nanoparticle suspension on thermal properties. The results show that adding non-fine particles to the base fluid greatly enhances heat transfer properties. Each of the nanofluids contains two unique nanoparticle concentrations. TiO_2/water has best heat transfer at its optimal concentration of nanofluids than Al_2O_3/water nanofluid at a certain number of Peclet, but Al_2O_3 /water nanofluid with hydrophilic nanoparticles has better heat transfer characteristics at higher concentrations of nanoparticles. Arsana et al. (19) investigated the volume fraction effect on heat transfer rate and effectiveness in shell and tube heat exchangers. Al_2O_3 was used on the cold fluid in fraction quantities of (%wt 0.5, 1, and 1.5). In a 90°C setting, the temperature of the fluid is used. According to the results of this investigation, the most effective mixed fraction nanofluid volume is 42%, with a heat transfer rate of 7061.93 Watts. The State mixture volume percentage without nanofluid had the lowest efficiency of 17.7% with a heat transfer rate of 5666.71 Watts (19,20). Fard et al. (22) use water-water and nanofluid-water streams to evaluate plate and concentric tube heat exchangers. As the heat stream, a ZnO/water nanofluid 0.5% was employed. Cong Qi et al. (23,24) are researching the pressure drop and thermal performance of TiO_2/water nanofluids in double tube heat exchangers. A smaller heat exchanger pressure drop is achieved by reducing the required tube length with increased heat transfer coefficients (25). Huang (26) examined a nearly 185% improvement in the tube side heat transfer coefficient enables a reduction in the length and flow rate of the heat exchanger, which lowers the pressure drop by 94%, the entire cost of the heat exchanger was reduced by more than 55% as a consequence.

Table 1.1 Illustrative table of the references used in the literature and their titles.

NO	Type of HEX	Year	Title	Critical Results
(27)	Double Pipe heat exchanger	2020	Thermal and exergy analysis of air-nanofluid bubbly flow in a double-pipe heat exchanger	$\Delta P = 8.9\ kPa$ ε = 64%
(28)	Different type of Heat Exchangers	2012	Application of nanofluids in heat exchangers: A review	heat transfer coefficient for water and TiO_2 Q = 8000 $W/m^2.k$ (Water) Q = 8244 $W/m^2.k$ (0.2 TiO_2) Q = 8300 $W/m^2.k$ (0.6 TiO_2) Q = 8500 $W/m^2.k$ (1.0 TiO_2) Q = 8330 $W/m^2.k$ (2.0 TiO_2)
(29)	Shell and Tube Heat Exchanger	2021	Numerical Study of Shell and Tube Heat Exchanger Performance Enhancement Using Nanofluids and Baffling Technique	$\Delta P = 540\ Pa$ $\eta = 20.1\%\ (water)$ $\eta = 20.5\%\ (1\%\ Al_2O_3)$ $\eta = 20.6\%\ (2\%\ Al_2O_3)$ $\eta = 20.7\%\ (3\%\ Al_2O_3)$ *η : thermal performance mean factor*
(30)	Different type of Heat Exchangers	2017	Experimental and numerical studyof nanofluid in heat exchanger fitted by modified twisted tape: exergy analysis and ANN prediction model	f = 0.22 (1.5% SiO_2) Nu = 180
(31)	Different type of Heat Exchangers	2018	Experimental research on stabilities, thermophysical properties and heat transfer enhancement of nanofluids in heat exchanger systems,	$\Delta P = 793\ Pa$ laminar flow $\Delta P = 6000\ Pa$ turbulent flow η =1.11% laminar flow η=1.05 % turbulent flow
(32)	Different type of Heat Exchangers	2013	Heat transfer from water to nanofluids in a concentric-tube heat exchanger: an experimental investigation	U= 470 $J/m^2.K$ (water) U= 540 $J/m^2.K$ (2% nanofluid) U= 560 $J/m^2.K$ (3% nanofluid)
(33)	Shell and Tube Heat Exchanger	2010	Heat transfer of nanofluids in a shell and tube heat exchanger,	U=3250$W/m^2.K$(0.75% Al_2O_3) h=9000$W/m^2.K$(0.75% Al_2O_3)
(34)	Shell and Tube Heat Exchanger	2020	The Effect of Nanofluid Volume Fraction to the Rate of Heat Transfer	ε = 42.2% Q = 7061 Watt U = 303.05 $W/m^2.k$

			Convection Nanofluid Water-Al_2O_3 on Shell and Tube Heat Exchanger	At 1.5 % of Al_2O_3 nanofluid
(35)	Different type of Heat Exchangers	2020	On the role of nanofluids in thermal-hydraulic performance of heat exchangers - a review,"	$\Delta P = 9000\ Pa\ (Al_2O_3\ nf)$
(36)	Different type of Heat Exchangers	2013	Heat transfer through heat exchanger using Al_2O_3 nanofluid at different concentrations	f = 0.0112 (2% Al_2O_3) f = 0.01055 (1% Al_2O_3) f = 0.01048 (0.7% Al_2O_3) f = 0.0104 (0.5% Al_2O_3)
(37)	Concentric tube and plate heat exchangers	2011	Numerical and experimental investigation of heat transfer of ZnO/Water nanofluid in the concentric tube and plate heat exchangers	Q = 2000 Watt U = 5000 W/$m^2.k$ (water) U = 6000 W/$m^2.k$ (ZnO)
(38)	Double tube heat exchanger	2019	Based on an experimental investigation of the flow and heat transfer properties of nanofluids in double-tube heat exchangers	Q= 2000 Watt (smooth) Q= 2500 Watt (corrugated) NTU= 0.47 (smooth) NTU= 0.62 (corrugated) ε = 0.332 (smooth) ε = 0.412 (corrugated) $\Delta P = 1900\ Pa\ (smooth)$ $\Delta P = 1200\ Pa$ (corrugated) *(Using TiO_2-H_2O nanofluid)*
(39)	Shell and Tube Heat Exchanger	2016	Application of nanofluids for the optimal design of shell and tube heat exchangers using genetic algorithm,	$\Delta P = 31500\ Pa$ $(genetic\ algorithm)$
(26)	Plate heat exchangers	2016	Plate heat exchanger hybrid nanofluid mixture effects	h= 9500 W/$m^2.k$ $\Delta P = 9000\ Pa\ (Al_2O_3\ nf)$
(40)	Double Pipe heat exchanger	2019	ε-NTU analysis of turbulent flow in a corrugated double pipe heat exchanger: A numerical investigation	f= 0.26 ε = 0.22 NTU= 0.23

** **f**: friction factor, **ε** : effectiveness, **NTU**: number of transfer units, **ΔP** : pressure drop, h: enthalpy, **U**: overall heat transfer, **h**: enthalpy, **η**: heat transfer enhancement, **N**u: nuselt number.

1.2 Aim and Scope of the Study

Due to the increasing use of heat exchangers in recent years, especially in the fields of energy, industry, and production, numerous academics have directed to reduce the entropy generation and increase the transfer efficiency of the heat exchangers. When researching most studies in this field, there are found that researchers have relied on the use of nanoparticles. Nanoparticles that mix with some liquids this mixture is called nanofluids, and it has been observed that nanofluids have a positive effect in improving the work of the heat exchanger. This thesis uses three heat exchangers: plate heat exchanger, double pipe heat exchanger, and shell and tube heat exchanger and for the same heat capacity. SiO_2/water nanofluids are used as a coolant fluid, then the results will be compared to water as the main coolant. In addition, a comparison will be made to make the exchanges between them in terms of reducing entropy generation, increasing efficiency, and the number of units transferred using the NTU and the entropy generation minimization method. In the thesis study, an experimental setup of 3 heat exchangers was constructed, and the performance of the heat exchangers was checked relatively by running the experimental setup for different parameters. In the thesis study under the title "Review of the literature." In this study, studies are mentioned in the literature on heat exchangers, nanofluids, and nanofluids used in heat exchangers. In the "Theoretical Foundations" section of the study, the theoretical foundations are explained in detail. The " Methods and Materials " part of the study explains the experimental setup and calculation method. In the heading "Results" of the study, the outputs obtained using the experimental data will be examined and interpreted comparatively. In the heading "Conclusions" of the study, the results are interpreted in general terms, and suggestions that could form the basis for further studies will be made.

2. THEORTICAL FOUNDMENTALS

2.1 Nanofluids

Changes in flow shape, boundary conditions, or the fluid's thermal conductivity can all help passively improve heat transfer by convection. Many strategies have been proposed to enhance the fluids' ability to transmit heat. Researchers have also attempted to boost the thermal conductivity of base fluids by suspending micro- or larger-sized solid particles in fluids because solids have a greater thermal conductivity than liquids, as shown in Table 2.1. Since Maxwell's theoretical theory was published more than a century ago, there have been a number of theoretical and experimental investigations of suspensions containing solid particles (41). There is, however, no reliable mechanism to prevent the massive size and density of the solid particles from causing them to settle out of suspension. Such suspensions instability increases erosion risk and flows resistance. Therefore, the commercialization of fluids containing dispersed coarse-grained particles has yet to occur.

Table 2.1 Different solids' and liquids' thermal conductivities

Type	Material	Thermal Conductivity (W/m.K)
Metallic solids	Copper	401
	Aluminum	237
Nonmetallic solids	Silicon	148
	Alumina (Al_2O_3)	40
Metallic liquid	Sodium (644 K)	72.3
Nonmetallic liquids	Water	0.613
	Ethylene Glycol (EG)	0.253
	Engine Oil (EO)	0.145

Thanks to modern nanotechnology, processing and producing materials with average crystallite sizes of less than 50 nanometers are now possible (42). Nanofluids provide fascinating new options for enhancing heat transfer performance, making them fluids for heat transmission in the future when compared to pure liquids. In terms of features, they are anticipated to perform better than conventional heat transfer fluids and fluids containing tiny metallic particles (41). Furthermore, nanofluids have the ability to improve properties linked to abrasion over conventional solid/fluid mixtures (43). As a result, these equations are only valid for a limited number of nanofluids and parameter ranges. Before generic models can be built and confirmed, more experimental and theoretical research is required.

Table 2.2 Historical equations of nusselt number

Ref.	Nanofluids	Correlations
(44)	Al_2O_3-water, TiO_2-water, turbulent	$Nu = 0.021Re^{0.8}Pr^{0.5}$
(45)	Al_2O_3-water, pool boiling	$Nu = cRe_b^m Pr^{0.4}$
(46)	CuO-water, turbulent	$Nu = 0.0059\left(1 + 7.6286\, \emptyset_p^{0.6886}\, Pe_p^{0.001}\right) Re^{0.9238}\, Pr^{0.4}$
(47)	Graphite in transmission fluid, graphite-synthetic oil mixture, laminar	$Nu = cRe^m Pr^{1/3}(\frac{D}{L})^{1/3}(\frac{\mu_b}{\mu_\infty})^{0.14}$
(48)	Turbulent	$Nu = \frac{(f/8)(Re-1000)Pr}{1+\delta_\emptyset^+(f/8)^{1/2}\left(Pr_\emptyset^{2/3}-1\right)}$
(49)	Al_2O_3, Newtonian laminar, natural convection	$Nu = \frac{4\sqrt{5}}{3\Delta_{nf}}\left[\frac{\beta_r k_r^4 Gr_b}{378V_r^2(9\Delta_{nf}-5)}\right]_{\frac{1}{4}}$

Newtonian Al_2O_3/water nanofluids were examined by Polidori et al. (50) using the integral formalism approach to study the natural convection heat transfer in a laminar external boundary layer.

2.1.1 Nanofluids Application Area

The role that nanofluid plays in all applications significantly impacts the creation of next-generation machinery for a range of technical and medicinal uses. Some of the applications are covered in the following sections (51).

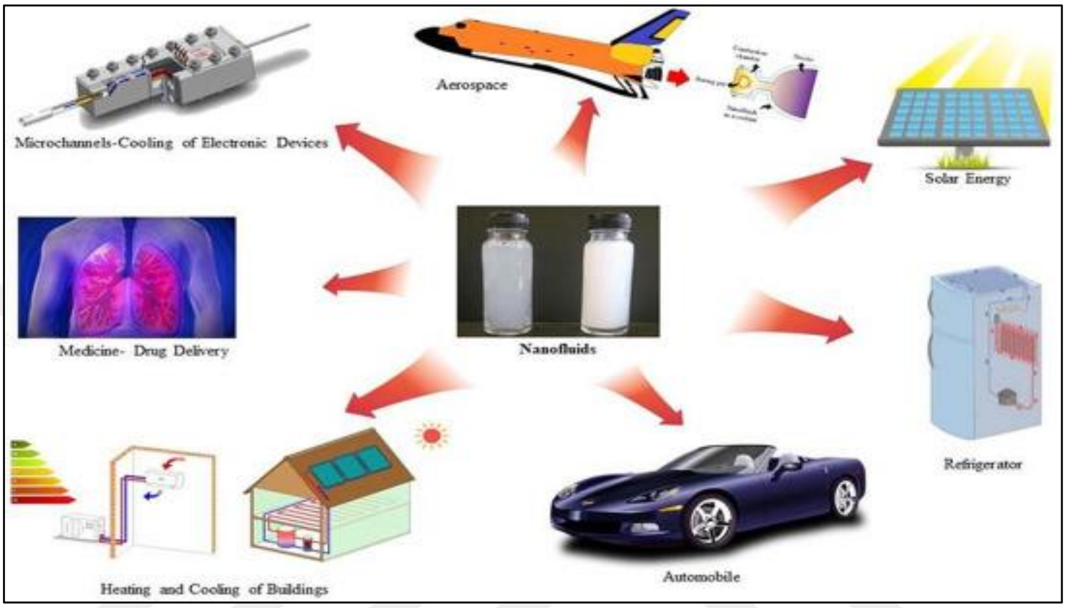

Figure 2. 1 Some of nanofluids applications (52).

2.1.1.1 Automobile Applications

To create nanofluids, nanoparticles and nanotubes are added to conventional engine coolants (ethylene glycol and water combination) and lubricants. This increases thermal conductivity, potentially increasing heat exchange rates and fuel efficiency (53). The vehicle's kinetic energy is dispersed by the heat produced during braking, which permeates the brake fluid in the hydraulic braking system (54), and the specifications for brake oil are now more stringent. To create CuO and aluminum-oxide-based braking nanofluids, the arc-submerged nanoparticle synthesis method and the plasma charging arc system was applied (55). The two kinds of nanofluids outperform conventional brake fluid in terms of conductivity, viscosity, and boiling point (56). The nanofluid brake oil's superior boiling point, conductivity, and viscosity will lessen the possibility of vapor-lock and increase driving safety (57).

2.1.1.2 Biomedical Applications

Because some of nanoparticles can carry drugs or have antibacterial properties, nanofluids made out of these nanoparticles will likewise have these qualities (57). Organic antibacterial substances are notoriously unstable, especially when subjected to high pressures or temperatures. Electrochemical studies suggest that ZnO nanoparticles touch the bacterial membrane at high ZnO concentrations (58). Green technology was employed by Jalal et al. (59) to produce ZnO nanoparticles. Bacterial survival ratios decrease with time and at higher ZnO nanofluid concentrations (60). It was shown that the size of silver nanoparticles affected their antibacterial effectiveness. Antimicrobial properties of silver have been demonstrated at concentrations as 01.69 mug//milliLeters Ag (61).

2.1.2 History of Nanofluids

In recent years, With the speed of development and sophistication of technology, the demand for micro/nano-sized particle manufacturing technology has been increasing (62). Micro/nanoparticles are used in electronic devices, pharmaceuticals, cosmetics, food, textile materials, agriculture, civil engineering, and energy materials (63). Many methods have already been reported as techniques for producing micro/nanoparticles. Asirvatham et al. (62,64) show that for volume fractions of 2, 4, and 6, heat transfer is improved by 12.1%, 11.5%, and 11%, respectively. With the addition of merely 1.0% of nanoparticle to water or ethylene glycol (65),the Nussult number increased by 40%. At 1%, the heat transfer rate increased owing to a larger heat transfer surface area at greater volume concentrations, reaching its highest rise from 1.143 to 1.276 at a concentration of 2.5%"(66,67). Due to suspended particles increasing the mixture's thermal conductivity, a two plate heat exchanger added 37% points of heat exchange for every 1.0% weight (68). Numerous researchers have utilized experimental techniques to show how copper nanoparticle volume concentration affects heat transmission (69). the enhanced heat transmission rate for suspended nanoscaled particles with high Peclet numbers (70,71).

In addition to nanoparticle volume fraction and particle size, some papers assert that temperature also significantly affects thermal conductivity (72). In addition, several conditions were applied, including adding a water-soluble dispersant, a dispersant plus surfactant combination, and no surfactant at all, all at temperatures between 15 and 40°C. The results showed that nanofluids with additional dispersant and surfactant had the lowest thermal conductivity (73). The heat coefficient of an automotive radiator is increased by up to 7% at inlet temperatures of 37 to 49°C for 1 vol%. In a narrow tube, Al_2O_3, TiO_2, and CeO_2 nanofluid were cooled via axial conduction, according to research by Haghighi et al. (74) due to heat losses, tube wall temperatures remained constant throughout the studies at a low heat flux of 0.3 W. Tiwari et al. (75) looked at the heat transfer properties of a CeO_2 /water nanofluid in a plate heat exchanger. The outcome shows that the CeO_2 /water nanofluid's convective heat transfer coefficient improved due to an increase in thermal conductivity brought on by a reduction in thermal boundary layer thickness when compared to water.

The nanofluids viscosity at an around temperature 27°C. CuO/water nanofluid viscosity was found to be much greater than the theoretical values anticipated by the Einstein model because intermolecular water interactions were minimized by utilizing nanoparticles at extremely low volume fractions (76,77). The findings indicate that anoincrease in the nanoparticles volumetric percentage caused the dynamic viscosity of the nanofluid to rise concurrently with the fluid's mass velocity, boosting theoheat transfer rate exponentially up to 3.8% (78).

In experimental comparison with water, whose surface tension was calculated using the "pendant drop" approach, Pantzali et al. looked at how a nanofluid performed in a PHE. And nanofluids were discovered to have surface tensions that were on par with or higher than water without the need for a surfactant. Surface tension was decreased when a surfactant was employed to stabilize CuO and CNT nanofluids (79).

2.2 Heat Exchangers

Cost, efficiency, and environmental factors are essential in all thermal applications to meet energy requirements. Heat exchangers are essential elements of heat application systems (80). The most widely used ones are finned-tube heat exchangers (81). Examples are condensers and evaporators in cooling facilities, radiators in water-cooled engines, and condensers in thermal power plants and chemical plants. Energy saving in heat exchangers is possible by using energy efficiently and effectively and increasing heat transfer. Considering that the need for energy is increasing daily and energy resources are decreasing, it is better understood how important it is to increase heat transfer in heat exchangers. In this context, many studies have been made and continue to be done to increase heat transfer in heat exchangers (82). Several of the research' objectives on the improvement of exchange of heat in heat exchangers are reducing their weight and size, increasing the amount of heat transfer, and reducing the average temperature difference between the fluids to improve the overall efficiency. Determining the type of heat exchanger is the most critical decision in heat exchange problems (83). The basic principle for selecting the heat exchanger type is to choose the type of heat exchanger operating under similar process conditions, (84) so the engineer's experience is significant. If a heat exchanger operating under similar process conditions cannot be found while determining the heat exchanger type, performance parameters (temperature program, flow rates, pressure drops), heat exchanger size, pressure and temperature, construction materials, types and phases of fluids, contamination trends, cleaning, inspection, repair, availability and economic etc.

Table 2.3 Heat exchangers types according to the direction of the fluid (85).

	Cross flow	**Parallel flow**
Double pipe HEX	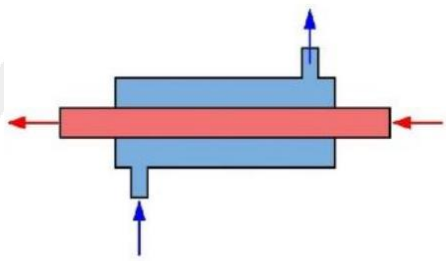	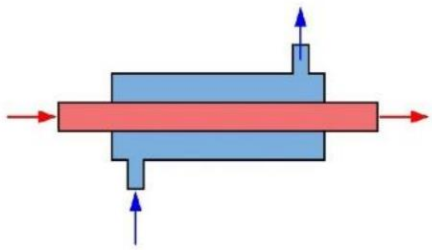
Shell and tube HEX	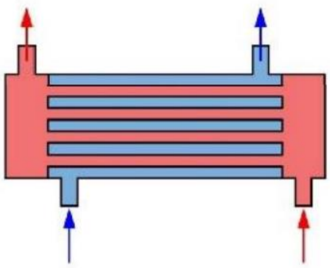	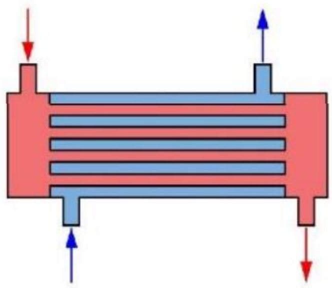

Plate heat exchanger	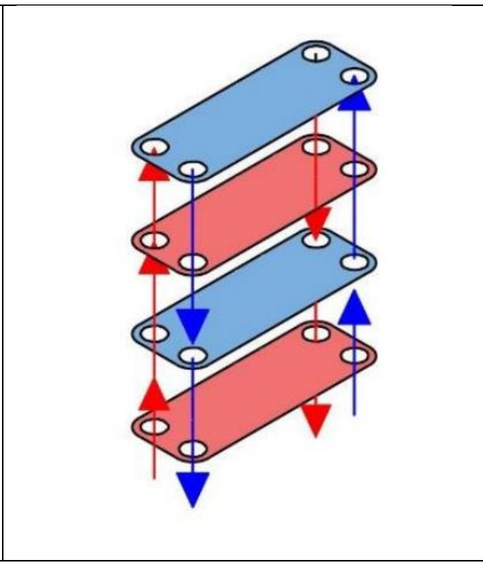	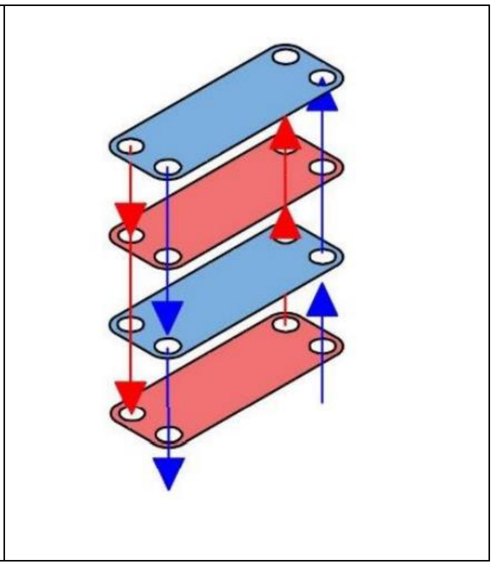

There are three tubular heat exchangers: shell-tube, double-pipe, and spiral-tube heat exchangers. Among these, the shell-and-tube heat exchanger has a wide range of applications compared to others due to its wide operating pressure and temperature range (86). These heat exchangers consist of channels with pipes of different sizes and are known for being easy to manufacture in different sizes and flow configurations (87).

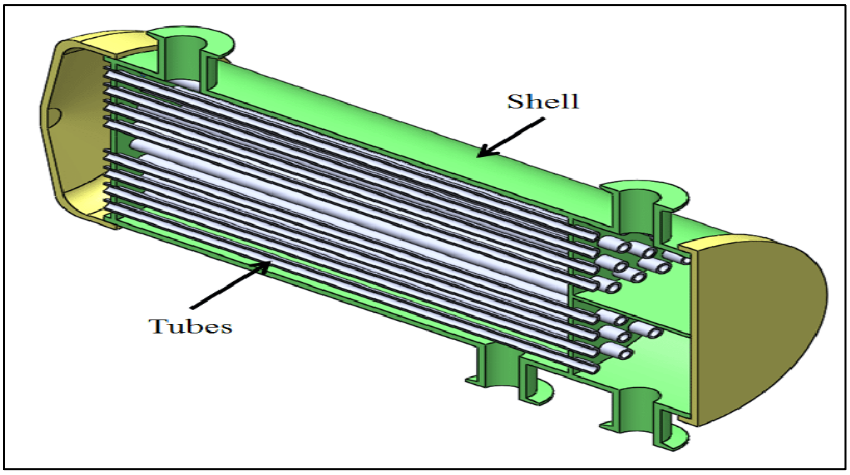

Figure 2.2 Shell and tube heat exchanger (88)

Double pipe heat exchanger is formed by concentrically placing a smaller pipe inside a large pipe. While one of the fluids flows from the inner pipe, the other flows from the outer pipe. They can be arranged in series or parallel to provide the desired pressure drop and temperature difference. The inner tube can be made in a single or multi-pipe form. The inner tube (or pipes) with axial fins can be used in cases where the heat transfer coefficient in the ring is low. Due to its versatility, inexpensive design and maintenance expenses, and low installation costs, double-tube heat exchangers are utilized in a variety of sectors (89). Due to its ease of configuration, maintenance, and cleaning, it is also suitable for high pressure fluids and high contamination conditions (90). Application areas of this heat exchanger; include heat recovery processes, air conditioning and cooling systems, chemical reactors, and food processes (91). However, the most significant disadvantages are their bulky designs and cost per unit transfer surface (92). Pourahmad and Pestle (93) conducted an experimental study on double-pipe heat exchangers by placing wavy strip turbulators on the inner tube. Their findings are significant advances in improving heat transfer properties. Gupta and Atrey (94) studied the performance evaluation of the counterflow heat exchanger for low-temperature applications; they found that counterflow heat exchangers are widely used in cryogenic systems due to their high efficiency. It has been stated that various losses, such as longitudinal conductivity along the wall, heat loss from surrounding leaks, and flow disruption, determine these heat exchangers' thermal performance. They went further in their research to comprehend the quantitative relationship between axial conductivity parameters and the decline of heat exchanger performance in the temperature ranges of 300–80 K and 80–20 K.

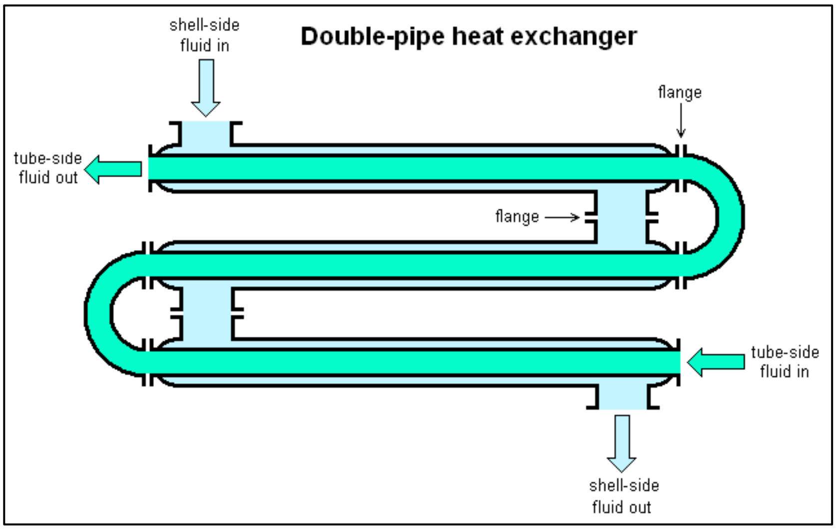

Figure 2.3 Double pipe heat excganger (95)

An array of channel plates make up a plate heat exchanger. The plate bundle is lined up between the upper and lower carrier bars, positioned between the moveable and fixed pressure plate (body), and secured with studs and bolts. The connectors (nozzles) on the stationary and mobile pressure plates are used to feed the fluids used in theoheat transfer process to the plate package (front and rear body) (96). Types of heat exchangers that can be used at low pressures in high pressure applications can be excluded from the selection immediately. Heat exchangers operating in a certain temperature range may also be the reason why they are not selected. It is more appropriate to choose the plate-type-heat exchanger, especially the gasketed plate type heat exchanger, when the operating temperature is below 200 °C.

At higher pressures and temperatures, one of the DPHE, STHE or welded PHE should be selected. In particular, the double-pipe heat exchanger is more suitable for small-capacity and high-pressure applications (97). Different types of heat exchangers have been optimized by researchers using various goals and techniques (98). Patel and Rao, for instance, optimized shell-and-tube heat exchangers, plate-fin heat exchangers, and regenerative heat exchangers using various optimization techniques (99).

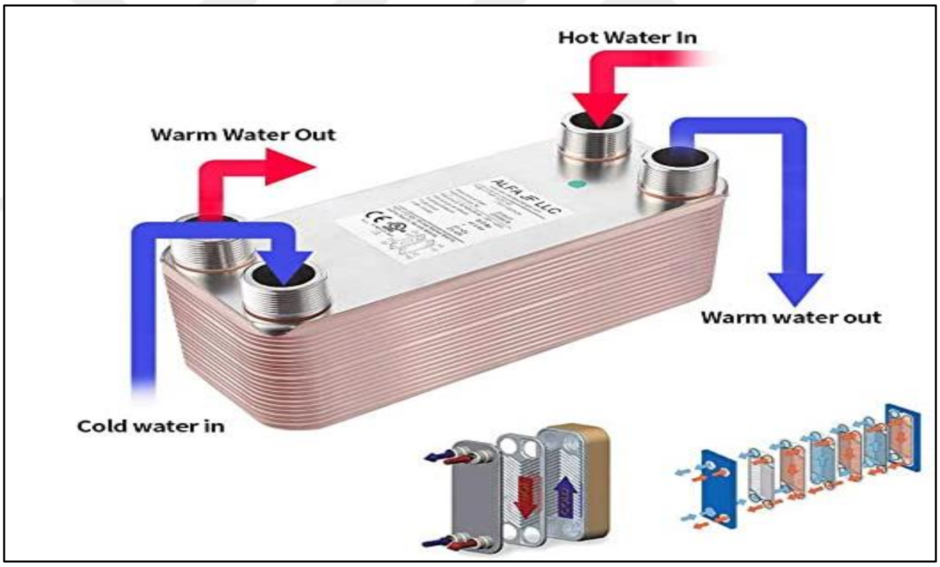

Figure 2.4 Plate heat exchanger (100)

2.2.1 Clasifications of Heat Exchangers

2.2.1.1 Tubular Heat Excangers

The heat exchanger is a crucial piece of process equipment that, roughly, is essential to all industries. To transfer heat between two or more fluids of differing temperatures, a heat exchanger is mostly used. This enables simple cooling and heating. Additionally, their industrial uses are quite diverse and include power production, electronics, chemical and food processing, waste heat recovery, air conditioning, and space applications (55,82).

Heat exchangers are generally characterized by their construction properties. Constructive properties of heat exchangers, which can be divided into main groups as tube, plate, fin and regenerative, will be given in this section, and their theoretical heat transfer and flow analyzes will be given in the following sections (103).

2.2.1.2 Straight Tube Heat Exchangers

A variation of the tube bundle heat exchanger is the straight tube heat exchanger. Wherever a quick heat transfer without pressure loss is required or where a viscous or polluted medium is employed, it can be found. Very thin single tubes are led straight through a large pipe for straight tube heat exchangers (104). Both the parallel flow and counterflow principles can be used to control them. During operation, the straight tube heat exchanger only produces a very little pressure loss. It can be designed horizontally or upright (vertically). The straight tube design makes it possible to employ polluted and viscous medium with no issues. Utilizing stainless steel will help reduce corrosion and deposits. As a result, the maintenance interval is significantly shortened (105).

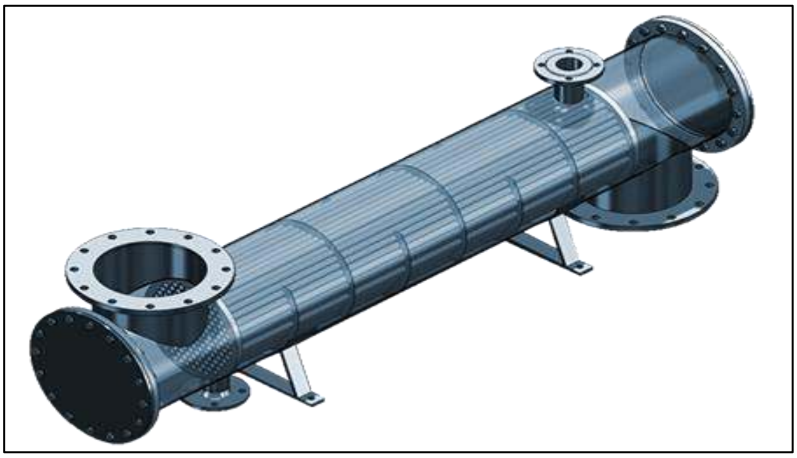

Figure 2.5 Straight tube heat exchanger (106)

2.2.1.3 Spiral Tube Heat Exchanger

A coil arrangement enclosed in a small shell, known as a spiral tube heat exchanger, maximizes both space and heat transmission efficiency. For strength and endurance, every Sentry spiral assembly incorporates tube to manifold connections that are welded. The coil assembly is put within a small shell after being soldered to a head. The spiral tube bundle's voids or gaps between the coils serve as the flow channel along the shell. A shell and tube design requires a larger footprint than a spiral because of its compact shape. The space requirements for tube bundle removal are drastically decreased because the tube bundle is coiled (107). Spiral tube heat exchangers employ less material when exotic material is needed because manifolds take the role of the channels, heads, and tubesheets in a traditional shell and tube design (108).

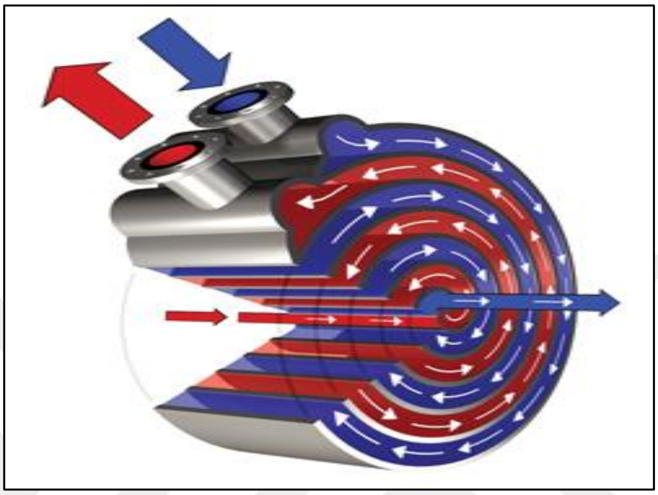

Figure 2.6 Spiral tube heat exchanger (109)

2.2.1.4 Shell and Tube Heat Exchanger

Tube and Shell heat exchanger is a device that transfers heat from one fluid to another without mixing or meeting two others that have different temperatures. By the heat transfer surface, fluids are kept apart from one another and do not combine. It has a wide range of applications and enhances the performance of the devices it is employed in. During manufacture, a heat exchanger's expansion is calculated, and the compensator that will be utilized is created using the results (110). According to customer requirements, custom-designed body and tube heat exchangers are constructed. The knowledgeable staff of the producers assists consumers in choosing materials (111). The choice of materials based on the fluid type and requirements, as well as the expansion calculation, are crucial for producing shell and tube heat exchangers. During production, the installation of the mirror and pipe differs depending on the material employed (112).

Another important issue in heat exchanger production is the form of screening. The body and tube heat exchanger, which is produced from carbon steel, stainless steel, duplex steel or special alloy materials, can also be produced from copper, brass or titanium materials (113).

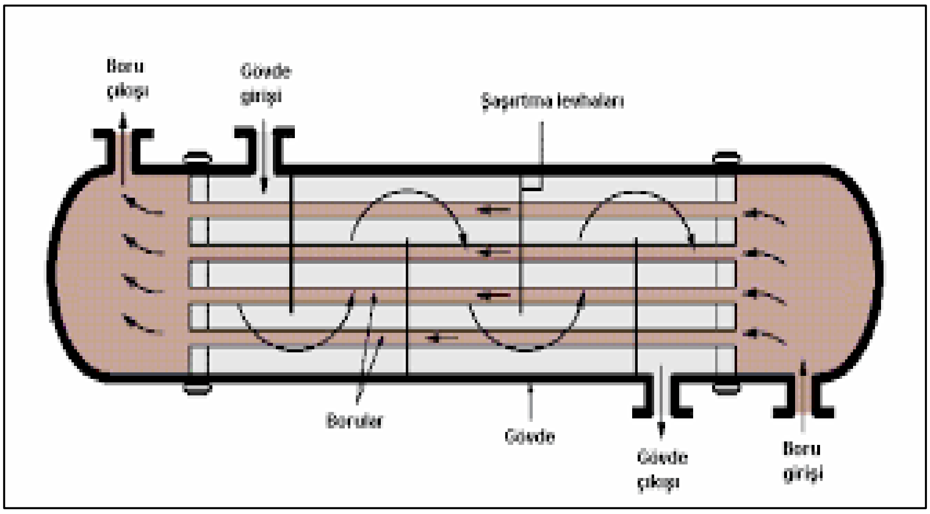

Figure 2.7 Shell-and-tube heat exchanger (114)

2.2.1.5 Plate Heat Exchangers

Thin plates are used during the production of plate type heat exchangers. The boards might be flat or protrude in a recessed pattern. High pressure, significant temperature, or high pressure or temperature variations will not damage this type of heat exchanger. They are separated into three categories: lamella, spiral plate, and gasketed. A package made of thin metal sheets can be used to create gasketed plate heat exchangers. These plates have perforations so that fluids can travel through each of their four corners (115). Fluids are directed with the help of effective seals, and mixing is prevented. Compression rods are used to compress it. The number of plates in the system can be increased or decreased to alter the thermal capacity as needed. In spiral plate heat exchangers, a spiral flow channel pair for the two fluids is created by helically winding two long metal strip sheets. The diameter of spiral plate heat exchangers is quite big as a result of these spiral turns (116).

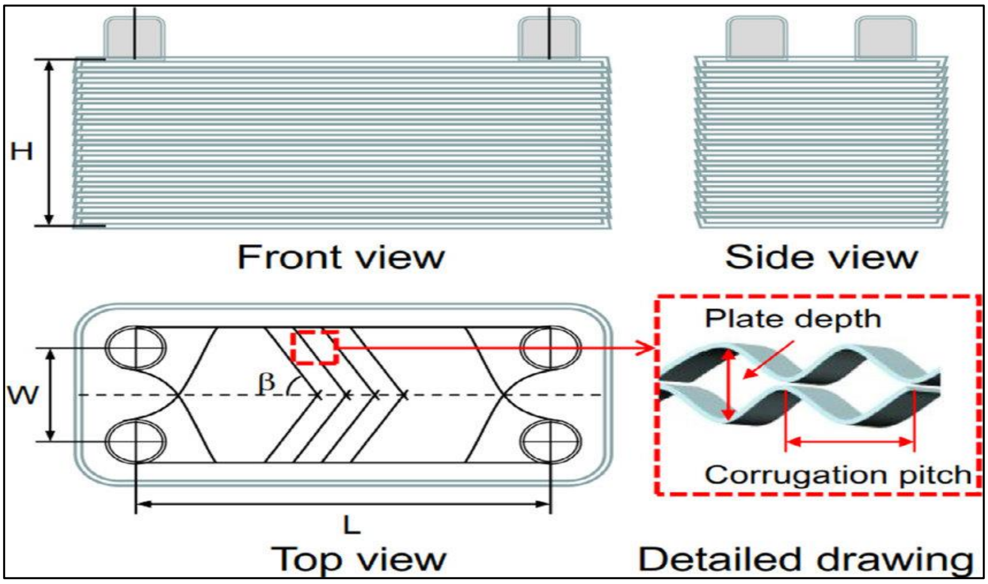

Figure 2.8 Schematic of the heat exchanger of plate (117).

2.2.1.6 Gasketed-Plate Heat Exchanger

Elastomeric gaskets are affixed to the plates of a gasketed-plate heat exchanger to seal the channels and direct fluid flow into other channels. The plate pack is compressed after being linked between the frame plate and the pressure plate by tightening bolts located there (118). The pressure plate and channel plates are located and supported, respectively, by lower and higher carrying bars that are also attached to the support column. The physical design of the gasketed plate heat exchanger makes it simple to clean and add or remove plates to adjust its capacity (119).

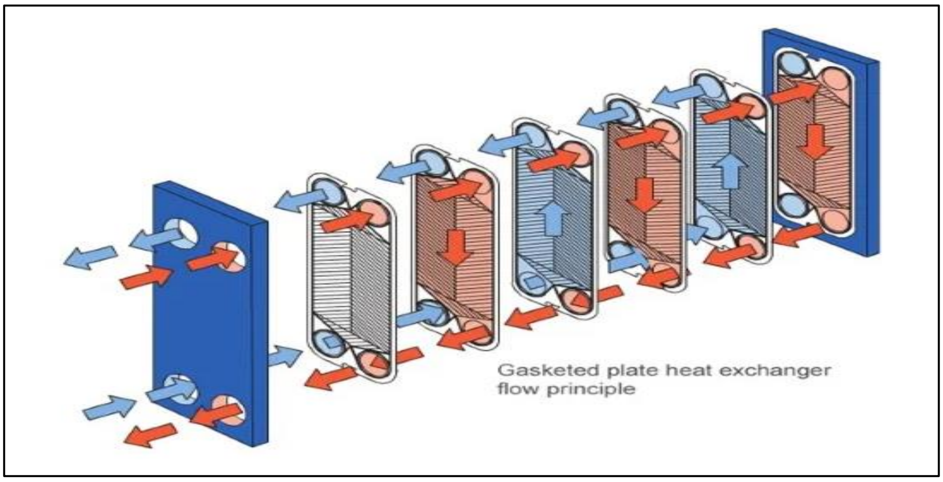

Figure 2.9 Gasketed plate heat exchanger (120)

Heat is transferred from the hot to the cold medium when the fluids go through the heat exchanger. Maximum heat recovery potential and extremely close temperature approaches are made possible by counter-current flow. It is also conceivable for temperatures to cross, which means that the hot outlet may become colder than the cold outlet (121).

2.2.1.7 Spiral Plate Heat Exchanger

A class of heat exchangers known as the spiral plate heat exchanger is really based on the type A spiral core. Welding seams and head configurations may be changed to generate different spiral heat exchangers. The spiral is appealing to various businesses and applications because of its adaptability (122).

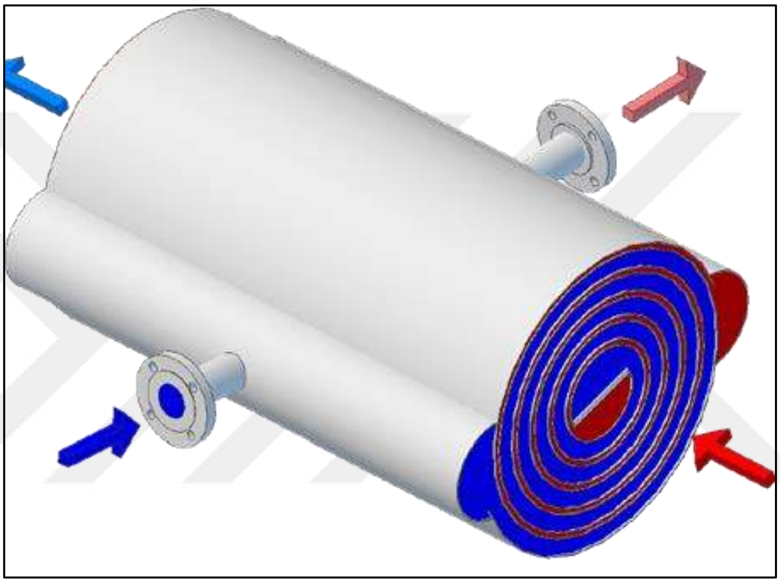

Figure 2.10 Spiral plate heat exchanger (123)

Spiral HEXs are spherical objects with two fluid-specific concentric spiral flow channels. The two media flow counters are now configured so that one fluid enters from the center and flows outward, and the other fluid enters from the exterior and moves inward. The channels have a homogeneous cross section and are curved. Combining pipes is not problematic (124).

Typically, one side of the product channel is open and the other is closed. Depending on the cleanliness of the heating or cooling medium, the channel can occasionally be blocked on both sides. The heat exchanger includes two connections for each channel, one in the middle and one on either side (125).

2.2.1.8 Lamella Heat Exchanger

A lamella heat exchanger is made up of an inner bundle of heat transfer devices and an outside tubular shell. These exchangers are made up of a series of longitudinally arranged flat tubes or rectangular channels made of thin plate channels or lamellae that are parallel and welded. Typically, the shell side flow only makes one trip around the plates, flowing longitudinally through the gaps between the channels. Lamella heat exchangers may be set up for real counter-current flow since there are no shell side baffles (126).

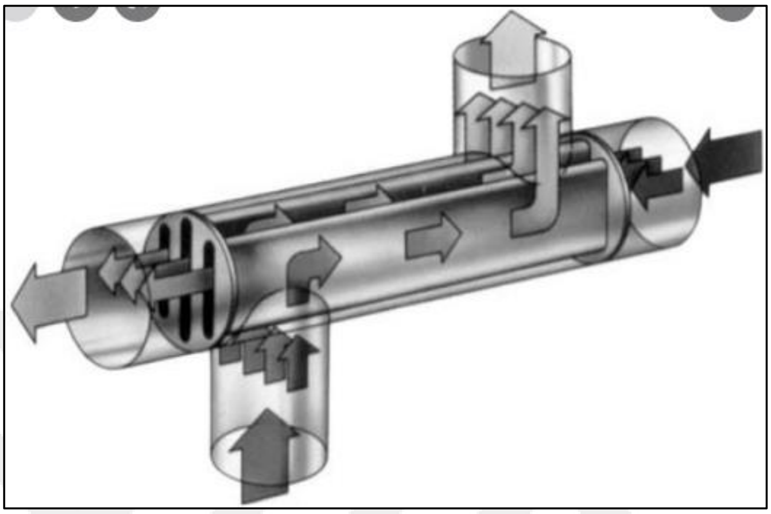

Figure 2.11 Lamella heat exchanger (127)

2.2.1.9 Finned Tube Heat Exchangers

A fin tube heat exchanger works especially well with an air heat exchanger. The liquid outside the tube, which is frequently air or another gas, obtains a significant amount of extra heat transfer surface area for a fin tube heat exchanger (128). The calculated heat transfer coefficients at surfaces within and outside the tubes are based on correlations discovered via experimentation. In order to assess how well fins transport heat, correlations are employed. Numerous sets of correlations are available for estimating the heat transfer effectiveness of longitudinal and transverse fins (129). By combining the bare tube area with the fin area and fin heat transfer efficiency, the effective outer heat transfer area is determined (130).

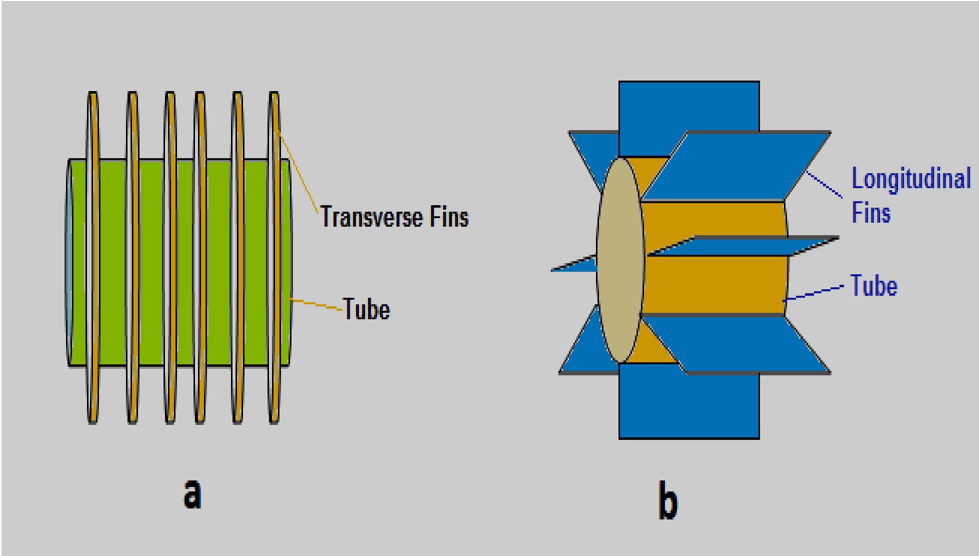

Figure 2.12 Finned tube heat exchangers, (a) Transverse Fins, (b) Longitudinal Fins (131)

2.2.1.10 Regenerative Heat Exchangers

A rotary total heat exchanger is a regenerative heat exchanger that recovers total heat or sensible heat from the exhaust air to the supply air through the rotation of the rotor. It is a typical energy-saving equipment for air conditioning that can contribute to the reduction of outdoor air load during cooling and heating in office buildings, general buildings, factories, etc., throughout the summer and winter (132). The rotary total heat exchanger consists of an aluminum rotor, a motor with a speed reducer, and a belt, and the rotor is driven at a low speed (20 rpm or less)(133). At this time, most of the heat (temperature and humidity) in the return air is collected in the rotor, and only the dirty air is discharged outside. On the other hand, outside air passes through the upper half of the rotor and is supplied to the room. At this time, the outside air continuously receives all the heat recovered from the return air and supplies it to the room. As you can see from the above, the rotary total heat exchanger can reduce the heat load of fresh outside air, so it is an energy-saving device that can greatly reduce running costs (134). This regenerator can be a component of a Stirling engine or other valveless system. Another setup results in output temperatures that change over time when the fluid is ducted via valves to various matrices during alternate working periods (135).

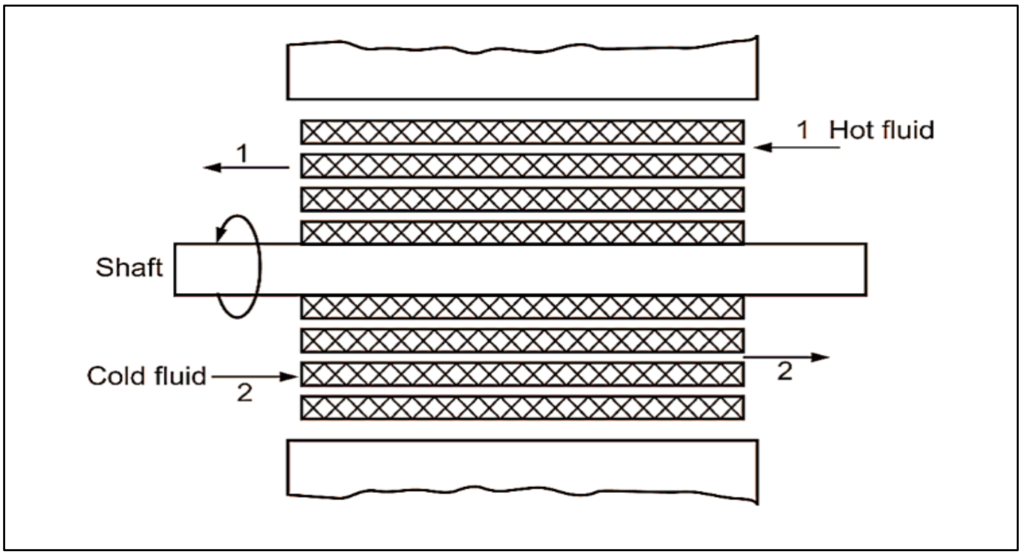

Figure 2.13 Rotary regenerative-heat-exchanger (136)

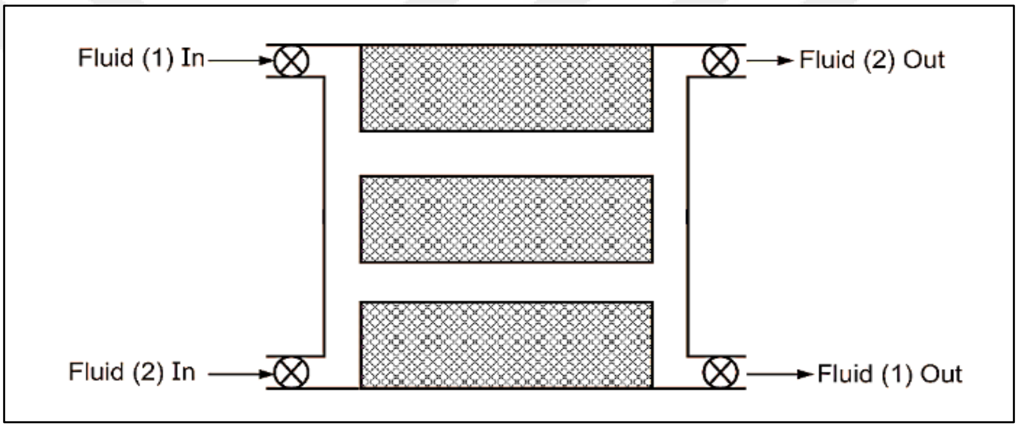

Figure 2.14 Fixed regenerative heat exchanger (137)

2.3 Entropy

The concept of Entropy, which is the second law of thermodynamics, was first defined in the literature by Rudolph Clausius in 1965 as a measure of disorder and uncertainty in a system (102). The concept of Entropy, which is widely used in physics, mathematics, and engineering sciences today, was adapted to information theory by Shannon (1948). The entropy method is used to measure the amount of useful information provided by the existing data (138).

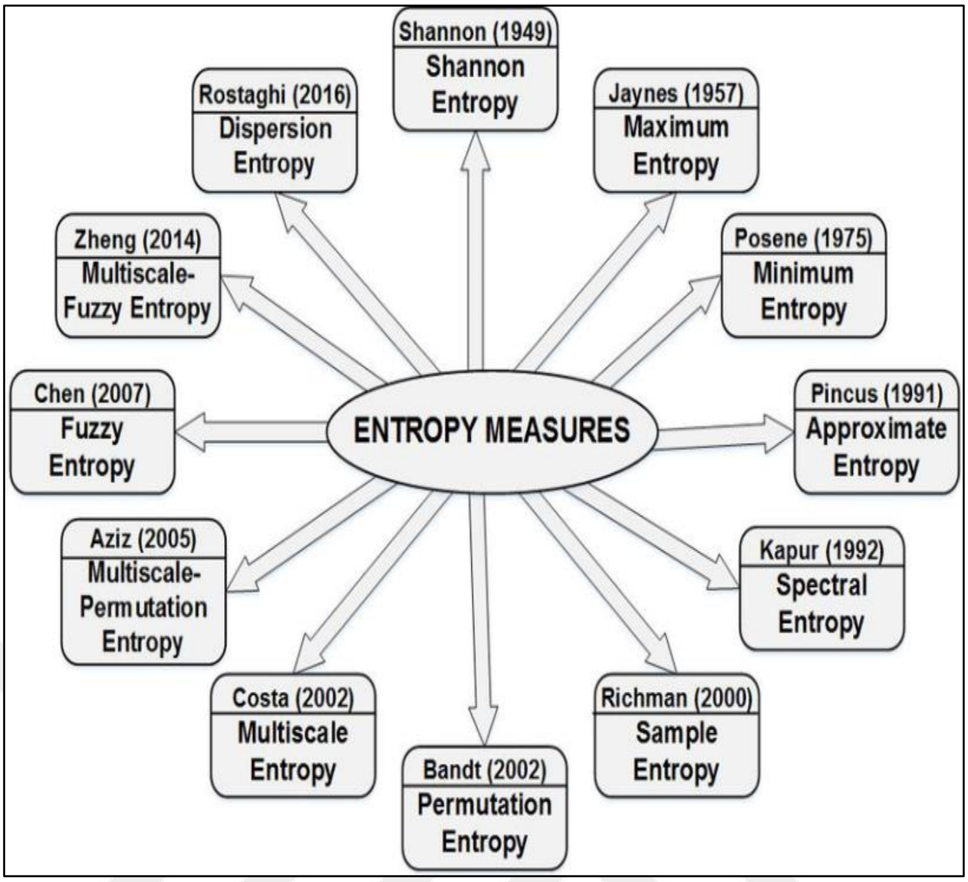

Figure 2.15 Entropy generation types (139).

2.3.1 Entropy Generation Caused by Finite Temperature Differences

Thermodynamic sweatproofing is significantly impacted by the temperature distribution in heat exchangers. By calculating the related entropy production, reverse strength may also be found. Work potential lost as a result of irreversibility during a process is referred to as irreversibility (also known as exergy destruction and lost work) (140). As entropy is produced, the impact of temperature variations on irreversibility may be described as follows. The entropy production for a heat exchanger that is thought of as an open, adiabatic system is given as:

$$\dot{S}g = \Delta\dot{S} = \dot{m}_1 \Delta s_1 + \dot{m}_2 \Delta s_2 \quad (1)$$

2.3.2 Entropy Generation Resulting from Fluid Mixing

Both the heat transfer process's thermodynamic efficiency and the heat exchanger's efficacy are reduced due to thermodynamic irreversibility and entropy formation caused by fluid mixing in a heat exchanger. Fluids that differ from one another in terms of composition and state characteristics tend to mix irreversibly. As a result, the pace at which entropy is generated depends on how different the mixing fluids are (141).

The irreversibilities connected to a mixing process are caused by:

1. the process of combining particles of different substances;
2. The exchange of energy between similar or dissimilar substances or within mixed substances.
3. Heat transfer between the environment and the substances being mixed,
4. Impacts of viscous dissipation.

Unbounded mixing reduces temperature inconsistencies at the fluid's cross section while obliterating the thermal potential. This process lowers the heat exchanger's efficiency and increases the formation of entropy.

2.3.3 Fluid Friction Entropy Generation

One of the leading causes of pressure loss in heat exchangers is fluid friction through the heat transfer surface. In many circumstances, mainly when incompressible liquids are used for heat transmission, the influence of the pressure drop is less significant than the temperature effect. Due to pressure losses in the ducts or tubes of heat exchangers, mechanical power is needed to pump the working fluids through each exchanger. If liquids are employed in the system, the pumping power will probably be less than it is for gases. Pumping power, which is sometimes referred to as a measure of fundamental energy, will be a crucial design parameter regardless of whether gases or air are employed in the system (142). Both skin friction and form drag should be considered when drawing the control volume at the system's inlet and outflow. Entropy created by such a flow equals the change in entropy that occurs along the flow route between the two sites (inlet and outflow).

2.4 Response Surface Method

Response surface modeling (RSM) is used to determine the value(s) that cause the response variable to be at its maximum or lowest and to show the influence of the factors (explanatory variables) on the response variable (143). This method uses several mathematical and statistical tools to describe the link between the response variable and the explanatory factors. Finding the variables that are believed to impact the response variables is the first stage in RSM. The response surface method employs experimental design, regression modeling, and optimization techniques (144). Finding the functional link between the explanatory factors and the actual response considering the experimental findings is one of the goals of response surface research.

Additionally, the goal is to identify the factors that make this function maximal or minimal. The response can be graphically depicted in three dimensions or as contour plots showing how the response surface is shaped. RSM is being applied to design optimization to cut the expense of pricy analytical methods and the numerical noise they produce (145). In terms of the coded variables, the first-order model often looks like this:

$$y = \beta_0 + \beta_1 x_1 + \beta_2 x_2 + \cdots + \beta_k x_k + \varepsilon$$

Where $\beta_0, \beta_1, \beta_2 \ldots \beta_k$ are the coefficients of the regression. The Least Square Estimation (LSE) approach is used to estimate the regression coefficients for the first-order model (146).

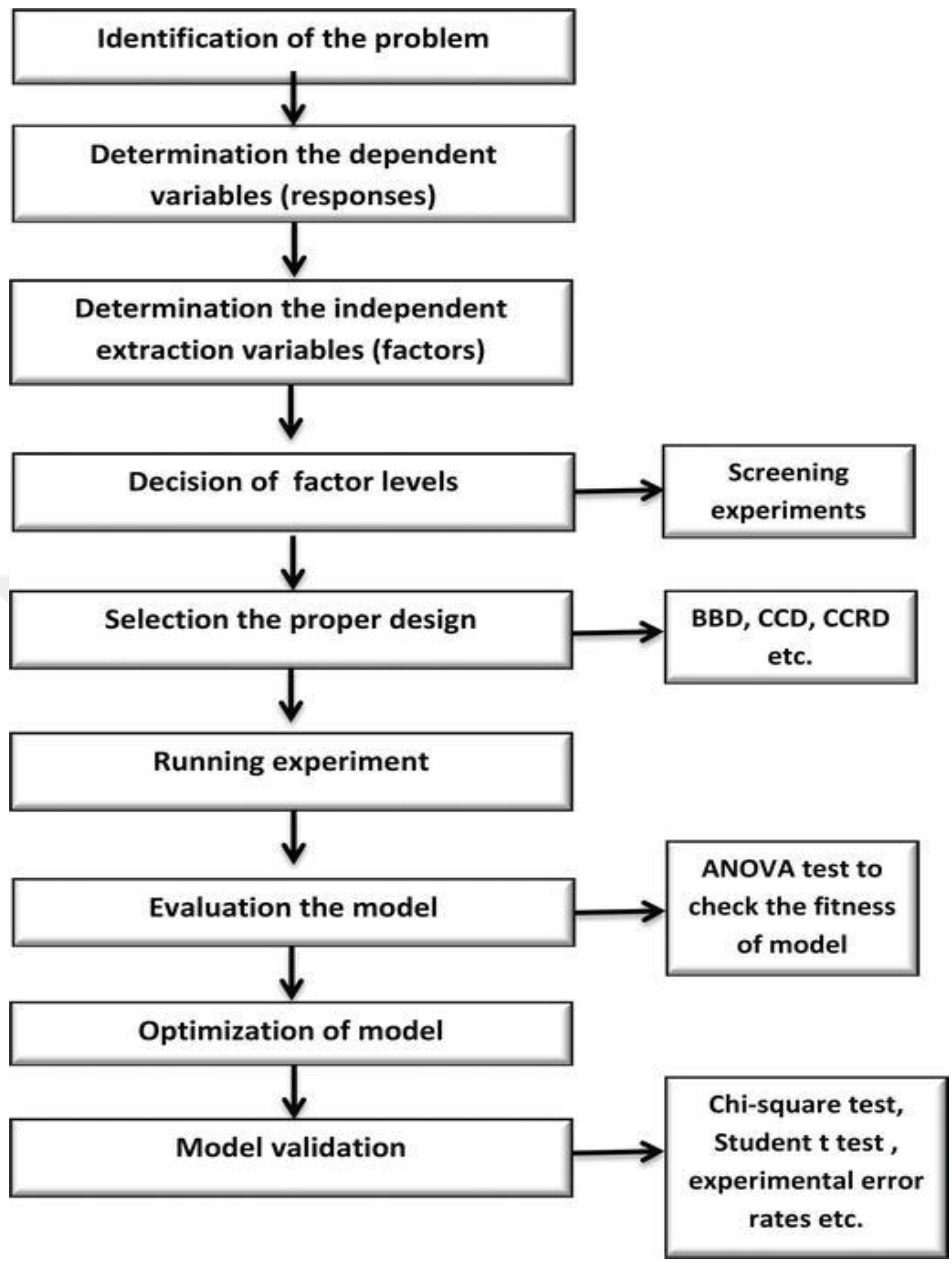

Figure 2.16 Steps for response surface methodology (147)

The most crucial component of RSM is the design of experiments (DoE). The DoE seeks to choose the most appropriate areas where the response should be thoroughly investigated. The design of experiments is mainly tied to the mathematical model of the process. The choice of experiment design thus has a significant impact on establishing the accuracy of the response surface creation. The RSM's benefits may be summed up as figuring out how the independent variables interact, mathematically modeling the system, and minimizing the number of trials to save time and money. Not all systems with curvature can be modeled by a second-order polynomial, as is commonly believed. Additionally, it is essential to do experimental validation of the model's estimated values (148).

3. MATERIALS AND METHODS

3.1 Materials

3.1.1 Experimental Setup and Equipment Details

Under this heading, A schematic and detailed picture of the test area and details of the system's equipment are presented. Picture 3.1 shows the real structure of the system and Figure 3.1 shows the experimental structure of the system. The system consists of two separate cycles. The first cycle is to heat the water to a specific temperature and then push it by the pump to the heat exchanger with a specific volumetric flow, after which the hot water returns to the heater for reheating. The second cycle pushes the nanofluid through the heat exchanger so that the heat is exchanged with the hot water in the first cycle, then the nanofluid returns to the cooler. These two cycles co-occur, and three heat exchangers are used one after the other. There are sensors to measure temperature and pressure before the entrances to the heat exchanger and after the exits.

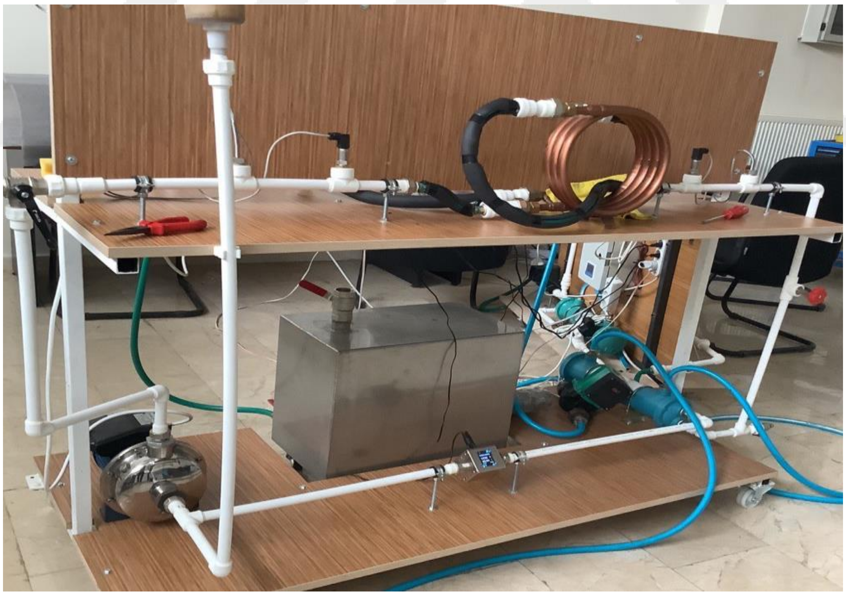

Picture 3.1 Real picture of structure system

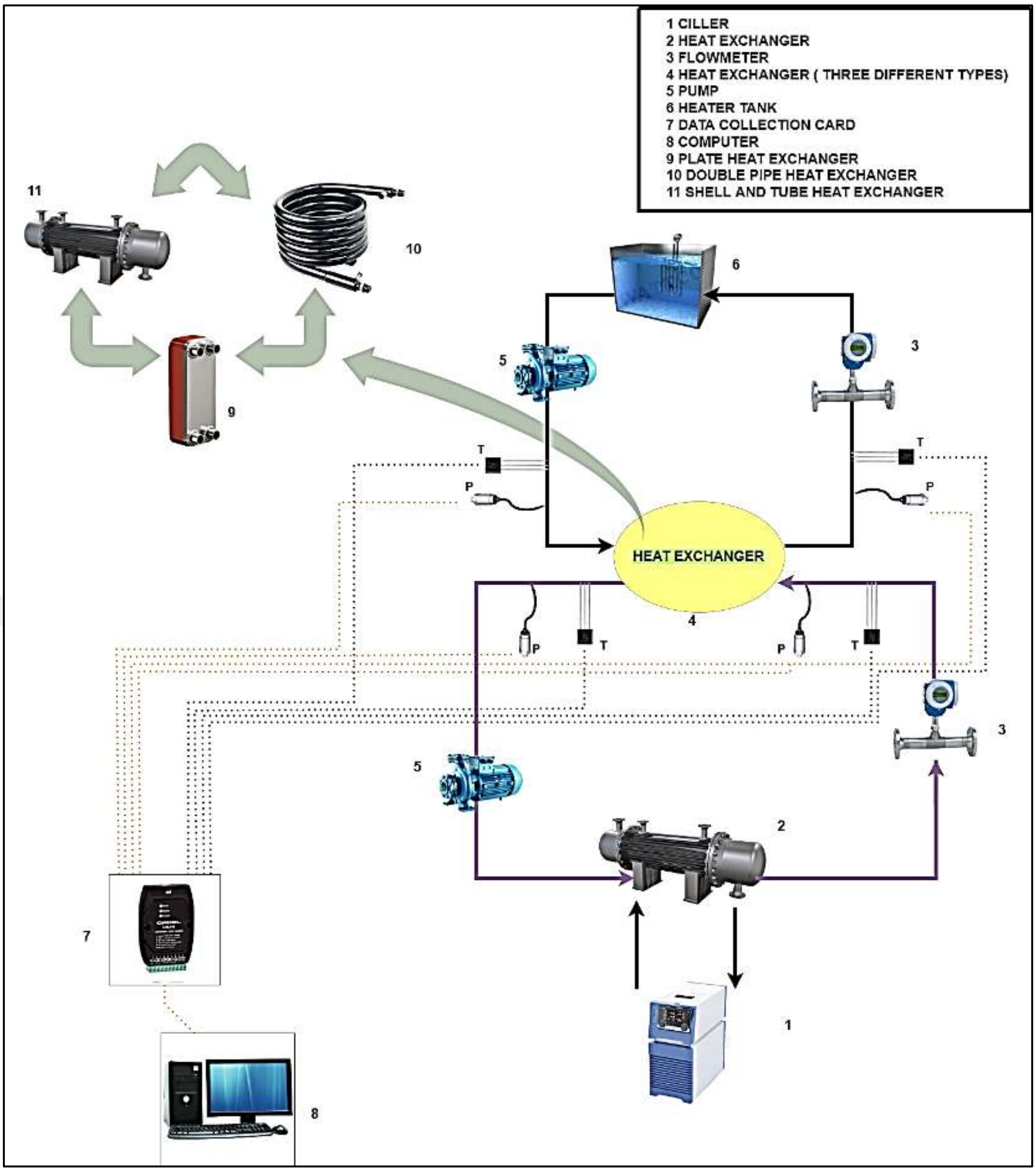

Figure 3.1 Experimental Setup and Equipment Details

3.1.2 Heat Exchanger Types in Study

3.1.2.1 Shell and Tube Heat Exchanger

It is a heat exchanger that conducts hot heat from one fluid to another. Tube heat exchangers often employ circular pipes. High pressures are not a problem for pipes with a circular section. High pressures are employed with the tube-type heat exchanger for this. Lower The main component of tube heat exchangers is a pipe. Pipe bundles are collections of steel or copper pipes. One fluid travels within the pipe while the other travels outside of it (149). Pipe diameter, number of pipes, pipe length, pipe pitch, and pipe arrangement can be changed.

For this reason, there is a great deal of flexibility in the design of tube heat exchangers (150). RelKon Lec Tube heat exchangers obtain the 90/70°C water required for heating by utilizing superheated water or steam. In high-pressure or temperature situations, tubular heat exchangers are preferred instead of gaskated or dangerous heat exchangers. Tube heat exchangers are a type of heat exchanger that can be used in all processes (151).

It is produced from carbon steel, stainless steel, copper, brass, and bafon pipe (152). They are designed considering the calcification and contamination conditions experienced in the pipe bundles. "U" pipe is preferred in steam systems. A straight pipe system with one side fixed, and the other floating mirror is preferred in oil systems. In this case, it is the selection of suitable gaskets for sealing that should be considered (153,154).

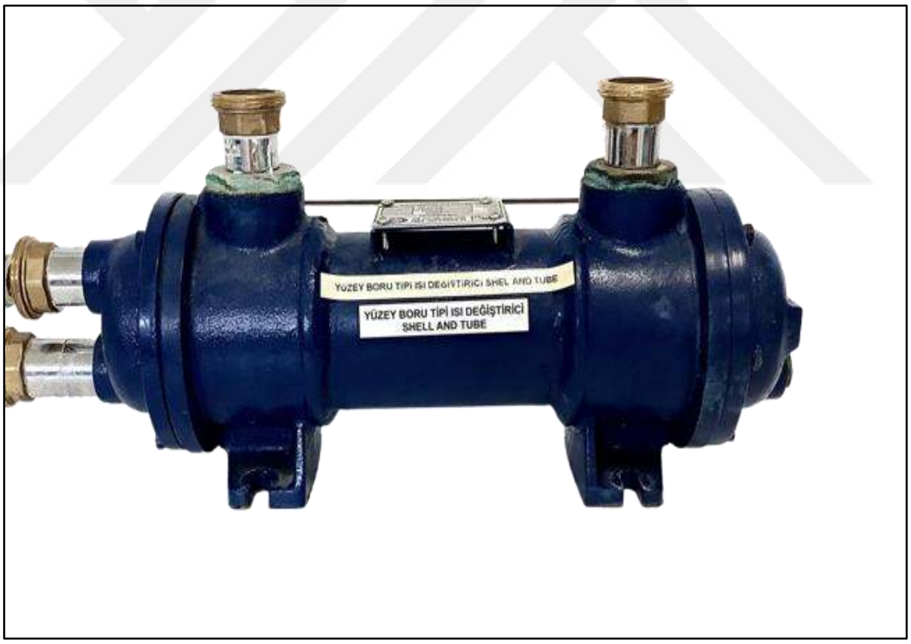

Picture 3.2 Shell and tube heat exchanger

3.1.2.2 Double Pipe Heat Exchanger

A liquid is in motion inside the pipe and farther along the annulus between the two pipes. The heat transmission surface is the inner tube's wall. The pipe is frequently folded and refolded several times to reduce the unit's overall size, as seen in the diagram on the left. The phrase "hairpin heat exchanger" is used in the configuration's heat exchanger schematic. The folding-back characteristic will always be visible, whether a hairpin heat exchanger tube has more than one inner tube or only one inside. Several heat exchanger manufacturers have announced the availability of buckling or finned tube twin heat exchangers (155). In flow finned tube heat exchangers, radial e is more frequently utilized and will always be used in place of transverse e.(30). The main benefit of a hairpin or double pipe heat exchanger arrangement is the ability to function in a more effective flow pattern, an actual countercurrent pattern. It will result in the twin-tube heat exchanger design with the highest overall heat transfer coefficient. In addition, heat exchangers with twin tubes and hairpins can withstand high temperatures and pressures. They can work with a temperature cross, where the cold-side outlet temperature is greater than the hot-side outlet temperature, and run on direct reverse current (156).

Picture 3.3 Double-Pipe Heat Exchanger.

3.1.2.3 Plate Heat Exchanger

Installation equipment called plate heat exchangers divides two fluids with different temperatures using plates, enabling the plates to exchange heat between the fluids (157). The effectiveness of heat transmission is plate heat exchangers' main advantage over other heat exchangers. Since the plates separating the two fluids are thinner than those made of alternative materials, the pace of heat transfer is accelerated, lowering the amount of heat lost during the transfer. Plate heat exchangers are effective and stop the accumulation of filth and residue in the systems they are utilized in. Additionally, it safeguards the system from any very high pressure that can develop during installation. Plate heat exchangers may serve various functions, such as a heating element, a cooling element, and a circuit separator, thanks to these characteristics that extend the life of the system they are utilized in (158). Regarding cost and efficiency, plate heat exchangers are more often used than tube-type heat exchangers. It even stopped the widespread usage of heat exchangers using tubes. Previously utilized in the food business. Plate heat exchangers are utilized in chemical processing, industrial purposes, the pharmaceutical industry, the food industry, the automotive sector, and other specialized applications. Additionally, plate heat exchangers, which excel in quality, safety, and ergonomic design, provide superb heat transfer options (159).

Picture 3.4 Plate Heat Exchanger

3.1.3 Technical Specification of Test Equipment

Several devices that were connected in a specific and accurate form were used for the purpose of obtaining the typical dimensions and controls determined by the parameters of this system, in Table 3.1 they are summarized preferably with their specifications.

Table 3.1 The devices and tools using in study

Equipment	**Picture**	Technical Properties

Chiller		**Brand:** B.E.O.-1,800 **Capacity of Cooling:** 1,800 W **Accuracy:**0.10% **Operating Range:** -20°C / +100°C
Shelloand tubeoheatoexchanger		Kontherm oil cooler, A=0.15 m²
Double Pipe Heat Exchanger		5/8"-7/8" A=3.14.DL =0.0967 m²
Plate heat exchanger		WEKO B3-14A-24 A=0,014 m² AxBxH: 77x35x207m
Flowmeter		**Brand:** Kobold **Type:** Magnetic Inductive **Measuring Range:** 0.04-10 l/min **Accuracy:**0.8%
Hot Line pump		**Brand:** Sumak SMT10-S, 0.75 kW **Operating Range:** 0-90°C **Type:** Peripheral

Cold Line pump		**Brand:** Wilo TOP-STG 25/7 **Operating Range**: -20°C-110°C **Type:** Circulation
Hot Water Tank	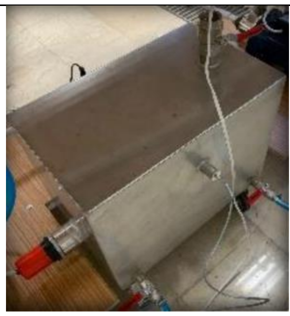	**Material**: Stainless Steel **Volume:** 90 L (60x50x30 cm3) **Resistance Power:** 5 Kw
Temperature Control for Hot Water		**Brand**: ENDA-442 **Type:** PID **Accuracy :**0.8%
Data Acquisition Card		**Brand**: Ordel UDL-100 **Accuracy:** ±0.2% **Measuring Range**: 750 ms
Thermocouple		**Brand**: Ordel **Type:** K type, Custom gear manufacturing **Measuring Range:** -200°C / +1200°C
Pressure Gauge		**Brand**: Keller **Type:** Piezoresistive **Measuring Range:** 0-4 bar **Accuracy:** < 1%

3.2 Methodology

3.2.1 Preperation of Nanofluids

By dissolving nanoparticles in a base liquid, nanofluids are formed. Because nanofluids require good dispersion, surfactants are occasionally added to improve their stability. Additionally, altering dispersed particles on the surface and applying significant force on scattered nanoparticle clusters may improve nanofluid stability. One-step and two-step procedures are the two simplest physical approaches for producing nanofluids. The chemical process is another novel technique for nanofluid production. The fraction of volumetric concentration is determined by Eq. 2.

$$\emptyset = \left[\frac{\frac{W_{np}}{\rho_{np}}}{\frac{W_{np}}{\rho_{np}} + \frac{W_{bf}}{\rho_{bf}}} \right] \times 100 \qquad (2)$$

W_{np} indicates how much a nanoparticle weighs., W_{bf} stands for the base fluid's weight., ρ_{np} indicates the nanofluid's density, and ρ_{bf} indicates the base fluid's density.

3.2.1.1 Two-Step Method

This technique of manufacturing is both low-cost and large-scale. In the two-step procedure, several technologies are employed to make nanoparticles, which are subsequently incorporated into the base liquid and distributed to create the required nanofluid. Nanoparticle aggregation is the two-step method's most severe flaw. Most scientists like using this technique to prepare nanofluids for investigation. Zhu et al. (160) (developed SiO_2/water nanofluid using a two-step procedure. In Figure 3.3, the two-step process is displayed.

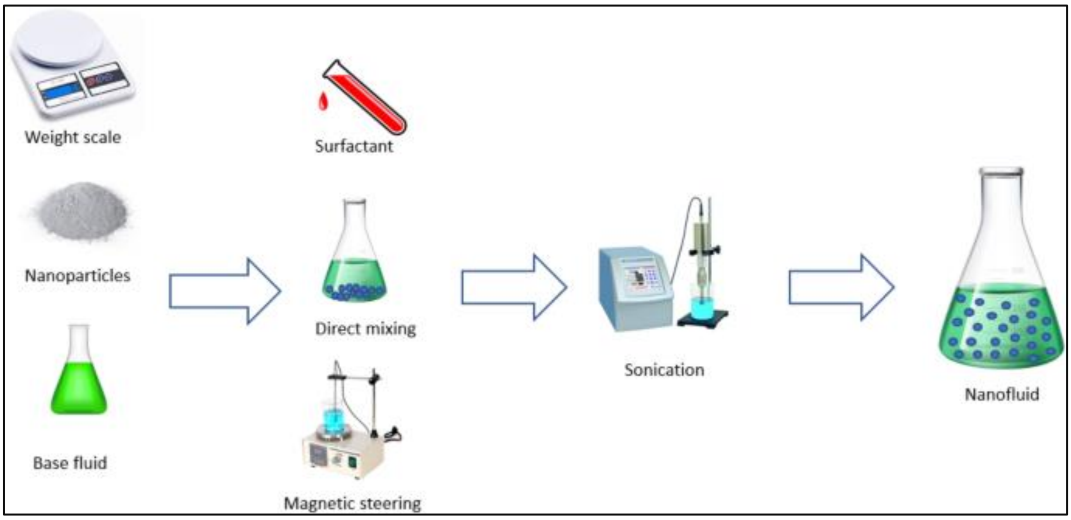

Figure 3.2 The Two-step procedure for nanofluids preparation (161)

3.2.2 Nanofluids Thermophysical Properties

An expression of the widely used correlations for calculating the thermophysical properties of the nanofluid, which are regularly discussed by several studies, is as follows:

3.2.2.1 Thermal Conductivity

the Wasp model provides an alternate formula for estimating thermal conductivity, which is stated as follows. (162,163).

$$k_{nf} = \left[\frac{k_p+2k_w+2\emptyset(k_p-k_w)}{k_p+2k_w-\emptyset(k_p-k_w)}\right] k_w \tag{3}$$

3.2.2.2 Viscosity

Brinkman (164) proposed an equation that is defined as follows to determine the suspension's viscosity.

$$\mu_{nf} = \frac{1}{(1-\emptyset)^{2.5}} \mu_w \tag{4}$$

Additionally, Wang et al. (165) suggested the following model to estimate the nanofluids viscosity:

$$\mu_{nf} = (1 + 7.3\emptyset + 123\emptyset^2)\mu_w \tag{5}$$

Additionally, Batchelor (166) developed a correlation to determine the viscosity of nanofluids containing spherical nanoparticles.

$$\mu_{nf} = (1 + 2.5\emptyset + 6.2\emptyset^2)\mu_w \tag{6}$$

There are a lot of equations, but Equation 4. will be used in the study to calculate the viscosity.

3.2.2.3 Specific heat and Density

The following definitions are used by Pak and Cho et al. to calculate the density and specific heat of the nanofluids. (167).

$$\rho_{nf} = \emptyset\rho_P + (1-\emptyset)\rho_w \quad (7)$$

and

$$Cp_{nf} = \frac{\emptyset\rho_{nf}Cp_P + (1-\emptyset)\rho_w Cp_w}{\rho_{nf}} \quad (8)$$

where Cp_{nf} isothe nanofluid's specific heat, Cp_P is the nanoparticles' specific heat, and Cp_w is the base fluid's specific heat.

Table 3.2 Thermophysical properties of nanofluids

Volumetric Contractions	Parameters	Equations	
Water	μ	y = -3E-09x^3 + 7E-07x^2 - 5E-05x + 0.0017	R^2 = 0.9995
	Cp	y = -0.0003x^3 + 0.0518x^2 - 2.5188x + 4214.7	R^2 = 0.9785
	ρ	y = -0.004x^2 - 0.0497x + 1000.6	R^2 = 0.9991
	k	y = -1E-05x^2 + 0.0021x + 0.5595	R^2 = 0.9997
0.1 %	μ	y = -3E-09x^3 + 7E-07x^2 - 5E-05x + 0.0017	R^2 = 0.9995
	Cp	y = -0.0003x^3 + 0.0517x^2 - 2.5164x + 4212.1	R^2 = 0.9785
	ρ	y = -0.004x^2 - 0.0496x + 1001.8	R^2 = 0.9991
	k	y = -1E-05x^2 + 0.0022x + 0.5603	R^2 = 0.9997
0.2 %	μ	y = -3E-09x^3 + 7E-07x^2 - 5E-05x + 0.0017	R^2 = 0.9995
	Cp	y = -0,0003x3 + 0,0517x2 - 2,5115x + 4207	R^2 = 0,9785
	ρ	y = -0.004x^2 - 0.0496x + 1004.2	R^2 = 0.9991
	k	y = -1E-05x^2 + 0.0022x + 0.562	R^2 = 0.9997
0.3 %	μ	y = -3E-09x^3 + 7E-07x^2 - 5E-05x + 0.0017	R^2 = 0.9995

	Cp	y = -0.0003x^3 + 0.0515x^2 - 2.5041x + 4199.2	R^2 = 0.9786
	ρ	y = -0.004x^2 - 0.0494x + 1007.8	R^2 = 0.9991
	k	y = -1E-05x^2 + 0.0022x + 0.5644	R^2 = 0.9997

3.2.3 Ɛ-NTU Method

If the liquid inlet and outlet temperatures can be anticipated using a simple energy balance or are known, the LMTD methodology can be used in heat exchanger research. If these temperatures are not known, the NTU method is used. The NTU method benefits all flow arrangements because a numerical solution of partial differential equations must obtain all other types of effectiveness. There is no analytical equation for LMTD or effectiveness (168). However, the effectiveness of each type can be presented. Hot water is in the tube, and cold fluid is in the shell in the heat exchanger's design. As with any industrial facility, the boiler supplies hot fluid. The rate of sensible heat transmission, or the amount of heat that heated and cooled water acquires, is as follows:

$$\dot{Q}_h = "C_h.\left(T_{h,in} - T_{h,out}\right)" \quad (9)$$

$$\dot{Q}_c = C_C.\left(T_{c,out} - T_{c,in}\right). \quad (10)$$

Assuming that the heat exchanger is insulated correctly, the rate of heat acquisition by the hot water will be equal to the rate of heat loss, and the capacity rate ratio can be expressed as follows (169):

$$C_r = \frac{C_{min}}{C_{max}} \quad (11)$$

Where:

$$C_h = m_h C_{P,h} \quad (12)$$

$$C_c = m_c C_{P,c} \quad (13)$$

To get the typical heat transfer coefficient, we using the equation given in Equation (14) using Equation (9) and Equation (10):

$$\dot{Q}_{avg} = \frac{\dot{Q}_h + \dot{Q}_c}{2} \quad (14)$$

The effectiveness of the heat exchanger may then be calculated using the equation below(170).

$$\varepsilon = \frac{q}{q_{max}} = \frac{c_h(T_{hi} - T_{ho})}{c_{min}(T_{hi} - T_{ci})} \quad (15)$$

The maximum possible heat transfer in a heat exchanger is defined as

$$q_{max} = C_{min}\left(T_{h,i} - T_{c,i}\right) \quad (16)$$

Here, Cmin denotes the lower of thermal capacities of cold and hot fluids.

Logaritm mean temperature difference is defined as:

$$\Delta T_{LMTD} = \frac{(T_{h,in} - T_{c,out})}{\ln\left(\frac{(T_{h,in} - T_{c,out})}{(T_{h,out} - T_{c,in})}\right)} \quad (17)$$

and the overall heat transfer coefficient is defined as:

$$U = \frac{\dot{\mathrm{Q}}_{\mathrm{avg}}}{A\,\Delta T_{LMTD}} \quad (18)$$

and the number heat transfer units (NTU) are defined as:

$$\mathrm{NTU} = \frac{\mathrm{UA}}{\mathrm{C_{min}}} \quad (19)$$

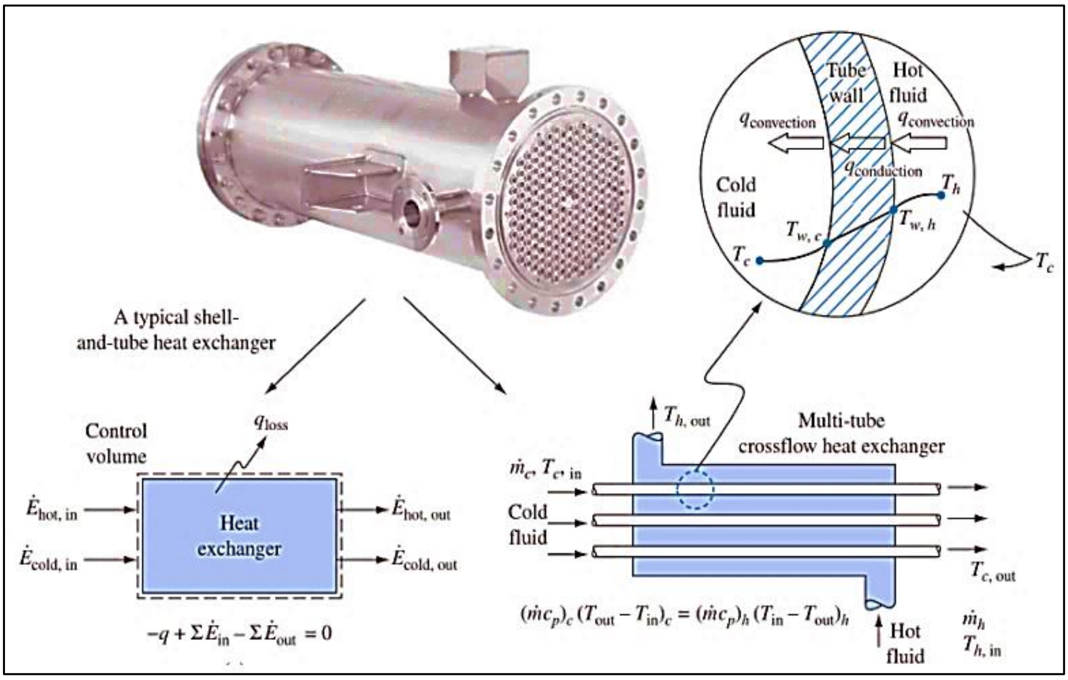

Figure 3.3 STHE diamentions calculations (170)

Tube side:

The Renold number for tube side is defined by (171)

$$Re_D = \frac{\rho u_m d_i}{\mu} = \frac{\dot{m} d_i}{\mu A_c} \tag{20}$$

And the heat transfer area is:

$$A_c = \frac{\pi d_i^2}{4} \frac{N_t}{N_p} \quad (0.5 \leq Pr \leq 2000) \tag{21}$$

And the Friction factor is defined by

$$f = 1.58 \ln (Re_D) - 3.28^{-2} \tag{22}$$

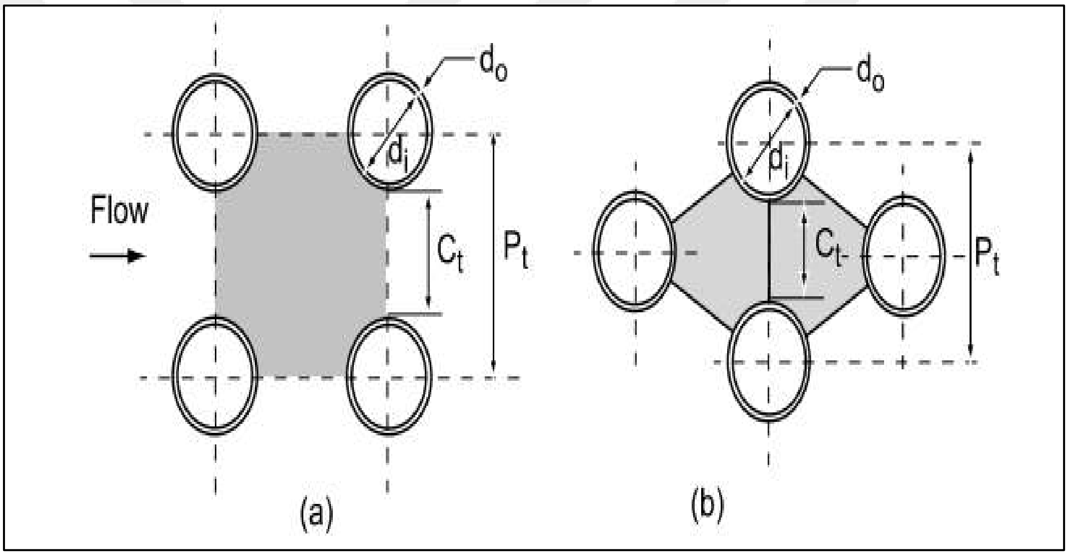

Figure 3.4 (a)\ Square-pitch-layout, (b) triangular-pitch-layout"(172)

Shell Side:

The Renold number for shell side is defined by:

$$Re_D = \frac{\rho u_m d_e}{\mu} = \frac{\dot{m} d_e}{\mu A_c} \tag{23}$$

And the heat transfer area is:

$$A_c = \frac{D_s C_t B}{P_t} \tag{24}$$

The Square pitch layout D_e is:

$$D_e = \frac{4(p_t^2 - \pi d_\circ^2/4)}{\pi d_\circ} \tag{25}$$

and for Triangular pitch layout is:

$$D_e = \frac{4\left(\frac{\sqrt{3}p_t^2}{4} - \pi d_\circ^2/8\right)}{\pi d_\circ/2} \quad (26)$$

3.2.4 Entropy Generation

According to the basic rule of thermodynamics, energy cannot be generated or destroyed; it can only change forms. The first law of thermodynamics concerns energy quality and transitions from one form to another regardless of quality. Losses always occur in natural cycles due to irreversibilities, and energy has a worse quality, according to the second rule of thermodynamics. As a result, entropy increases (173).

$$\dot{S}_{gen} = \frac{\partial S}{\partial t} - \sum_{in} \dot{m}s + \sum_{out} \dot{m}s - \frac{\dot{Q}}{T} \quad (27)$$

Where $\dot{\boldsymbol{m}}$ denotes the mass flow rate, **s** denotes the specific entropy, $\dot{\boldsymbol{Q}}$ denotes the heat flux across the system border, and **T** denotes the boundary temperature. Apply $\frac{\dot{Q}}{T} = 0$ and $\frac{\partial S}{\partial t} = 0$ for stationary state heat transfer and regard the current heat exchanger as an adiabatic system (174).

In plate heat exchangers, the hot and cold fluids are often made up of water, propylene glycol, ethylene glycol, motor oil, and other common fluids. Conventional fluids are changed out for fluids with better thermal conductivity to increase the efficiency of the plate heat exchanger. In common fluids, high thermal conductivity fluids known as nanofluids are made by scattering metal or metal-oxide solid nanoparticles. (175).

$$\dot{S}_{g,T} = \dot{m}_h \dot{c}_{p,h} ln\frac{T_{h,o}}{T_{h,i}} + \dot{m}_c \dot{c}_{p,c} ln\frac{T_{c,o}}{T_{c,i}} \quad (28)$$

$$\dot{S}_{g,p} = \left(\frac{\Delta P_h}{\rho_h}\right) \dot{m}_h \frac{ln\frac{T_{h,o}}{T_{h,i}}}{T_{h,o} - T_{h,i}} + \left(\frac{\Delta P_c}{\rho_c}\right) \dot{m}_c \frac{ln\frac{T_{c,o}}{T_{c,i}}}{T_{c,o} - T_{c,i}} \quad (29)$$

$$\dot{S}_g = \dot{S}_{g,p} + \dot{S}_{g,T} \quad (30)$$

Total entropy generation refers to the sum of creation of entropy due to friction and heat Eq.28 yields thermal entropy generation ($\dot{S}_{g,T}$), while Eq.29 yields frictional entropy generation ($\dot{S}_{g,p}$) (176).

3.2.5 Methodology of Response Surface

R.S.M. is a method that researchers Often use while planning and optimizing studies. The R.S.M technique is a computational and numerical method. for constructing and improving the experiment, allowing for the discovery of optimal parameters with the least amount of testing. Although R.S.M. was first used in empirical research, numerical studies have recently begun to use it as well. owing to its advantages, which include expanding experimental RSM and predicting nonlinear optimization processes while also reducing processing costs. is a method that researchers frequently use while planning and optimizing studies. (177).

A second-order model can significantly improve the optimization process when a first-order model displays lack of fit due to the interaction of variables and surface curvature. Generally speaking, a second-order model is:

$$Y = a_0 + \sum_{i=1}^{n} a_i x_i + \sum_{i=1}^{n} a_{ii} x_i^2 + \sum_{i=1}^{n} \sum_{i=1}^{n} a_{ij} x_i x_j \quad (31)$$

4. RESULTS

4.1 Effectiveness Results

Examining Figures 4.1, 4.2, and 4.3 reveals that the volumetric flow rate of the nanofluid progressively changes. SiO_2 nanofluid is employed atovolume concentrations of (%wt 0.1, 0.2, and 0.3). At nanofluid volume flow rates of (2, and 10) liters/min, respectively, the effectiveness of a 0.1% nanofluid, the DPHE, was increased by (%wt 10.89, 25.83) over the base fluid. At nanofluid volume flow rates of (2, and 10) liters/min, respectively, the effectiveness of the plate heat exchanger was increased by 10.49% and 27.71% over the base fluid. At nanofluid volume flow rates of (2, and 10) liters/min, respectively , the effectiveness of the STHE was increased by 7.42% and 21.40% over the base fluid. At nanofluid volume flow rates of (2, and 10) liters/min, the effectiveness was increased over the base liquid at 0.2% SiO_2 of the DPHE by 19.47% and 33.31%, respectively. With a nanofluid volume flow rate of (2, and 10) liters/min above the base fluid, the effectiveness of the PHE was increased by 16.28% and 36.72%. Additionally, at nanofluid volume flow rates of (2, and 10) liters/min, respectively, the effectiveness of the shell and tube heat exchanger was increased by 21.44% and 27.80% over the base liquid. At the nanofluid volume flow rates of (2, and 10) liters/min over the base liquid, the effectiveness was increased by 25.98% and 39.06% at 0.3% SiO_2 of the double pipe heat exchanger. At nanofluid volume flow rates of (2, and 10) liters/min, respectively, the efficacy of the plate heat exchanger was increased by 19.58% and 47.08% over the base fluid. Additionally, the effectiveness of the shell and tube heat exchanger was increased by 26.21% and 33.39%, respectively, with nanofluid volume flow rates of (2, and 10) liters/min over the base liquid. It has been shown that the effectiveness of the nanofluid improves with volume concentration and declines with volume flow rate. It should be noted that the PHE, followed by the DPHE, and the STHE, showed the highest rates of improvement in effectiveness.

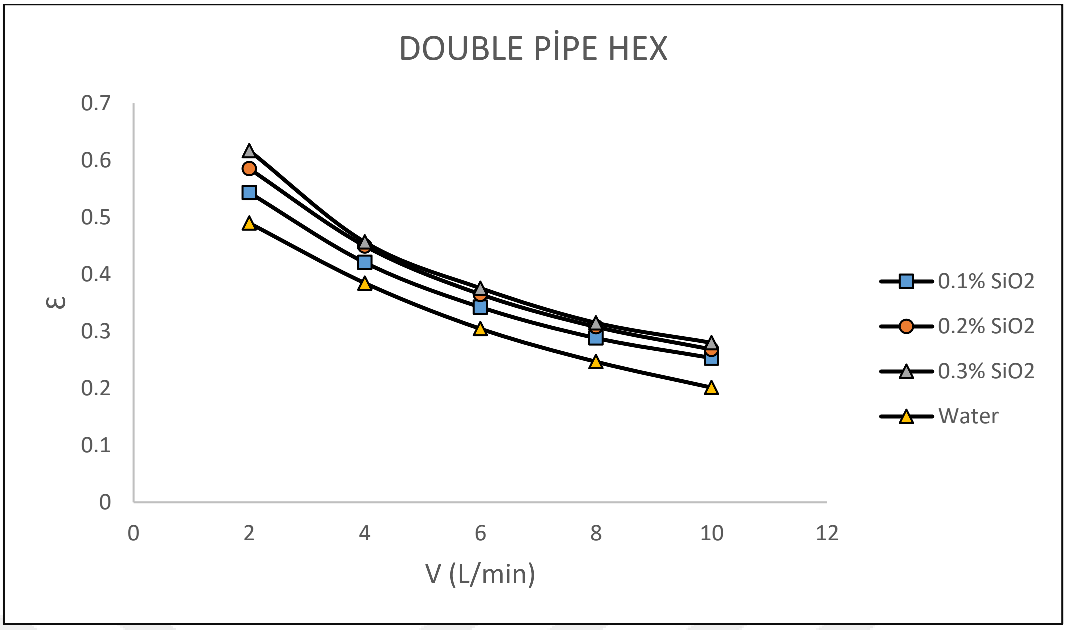

Figure 4.1 Volumetric rate and effectiveness results for DPHE

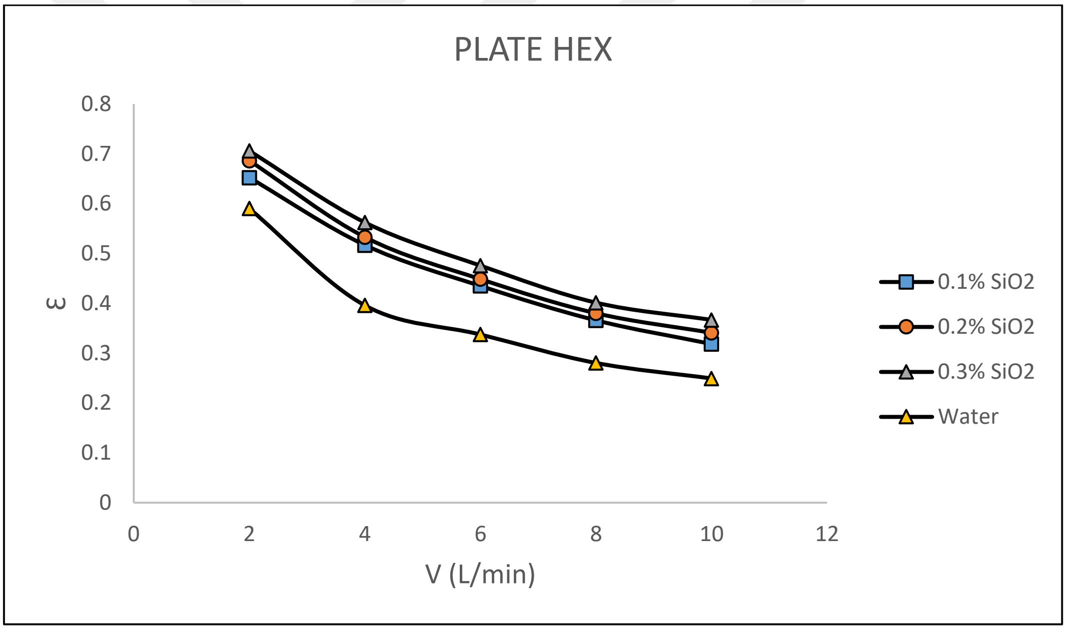

Figure 4.2 Volumetric rate and effectiveness results for PHE

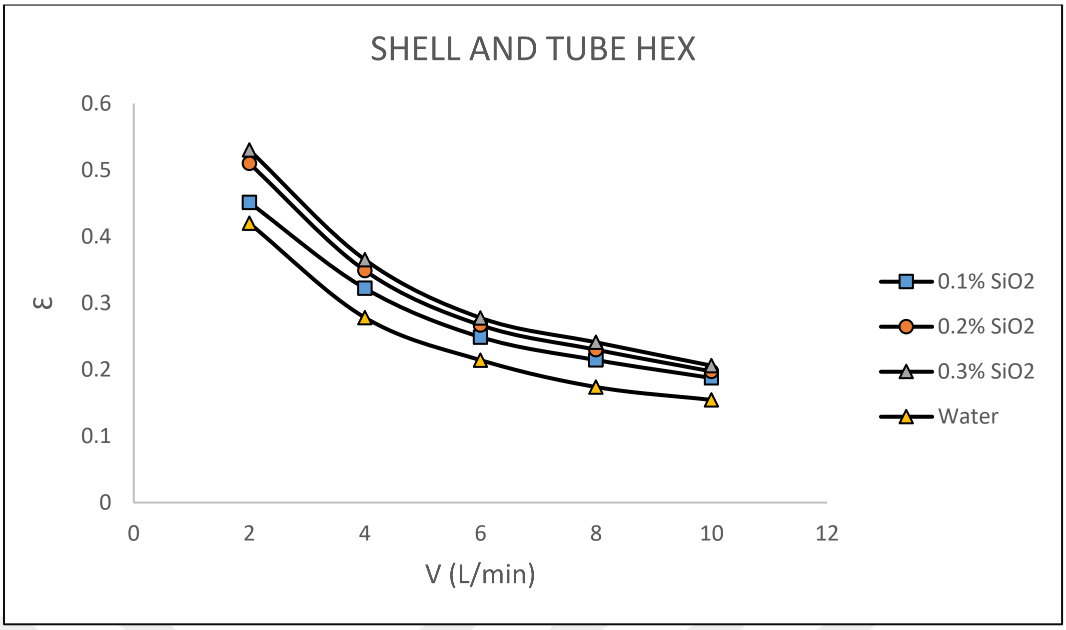

Figure 4.3 Volumetric rate and effectiveness results for STHE

When looking at Figures 4.1, 4.2, and 4.3, it is clear that the PHE, where the effectiveness appeared around 0.59 when using water without SiO_2, 0.65 at 0.1% SiO_2, 0.68 at 0.2% SiO_2, and 0.7 at 0.3% SiO_2 and a volume flow rate of 10 liters/min, achieved the highest values of effectiveness. The effectiveness of the DPHE appeared to be around 0.48 when using water without SiO_2, 0.54 at 0.1% SiO_2 and the last one is the STHE, where the effectiveness appeared to be about 0.41 when using water without SiO_2, 0.45 at 0.1% SiO_2, 0.50 at 0.2% SiO_2, and 0.53 at 0.3% SiO_2 at a rate of volumetric flow 10 liters/min.

4.2 NTU Results

In Figure 4.4 for the shell-and-tube heat exchanger, five volumetric flow rates of (2, 4, 6, 8, and 10) liters/min are used. Three volumetric concentrations of SiO_2 nanofluid are used (%wt 0.1, 0.2, and 0.3). Whereas the NTU values at 10 liters/min are 0.58, 0.69, 0.77, and 0.85 at (%wt 0.0, 0.1, 0.2, and 0.3) volumetric concentrations, respectively.

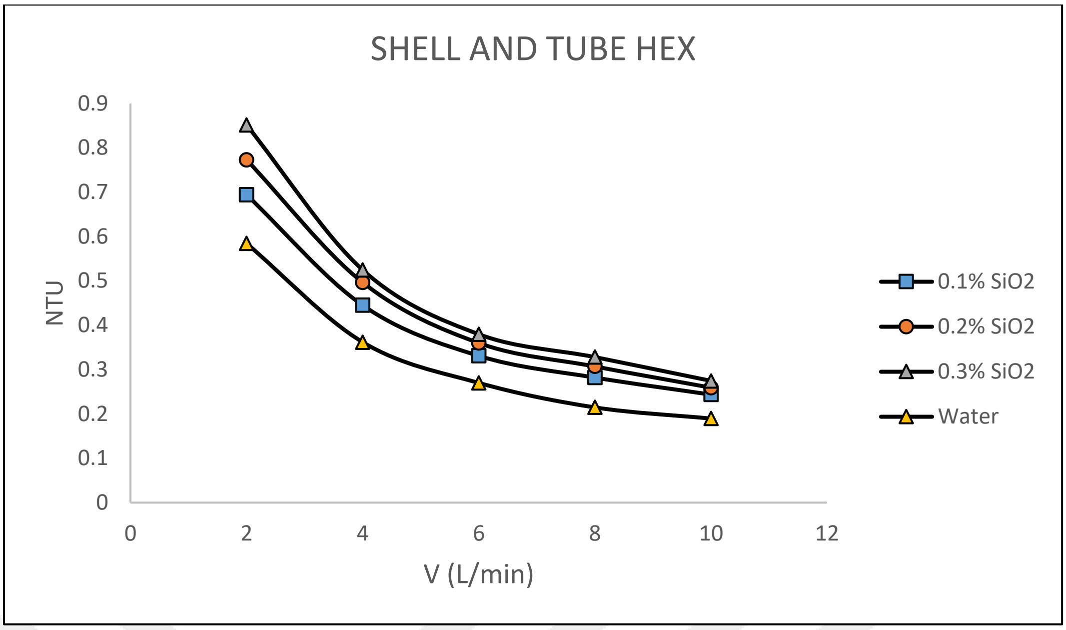

Figure 4.4 Volumetric rate and NTU results for shell-and-tube heat exchanger

In figure 4.5, five volumetric flow rates of (2, 4, 6 , 8 , and 10) liters/min are used for the double pipe heat exchanger. Three volumetric concentrations of SiO_2 nanofluid are used. (%wt 0.1, 0.2, and 0.3). Whereas the NTU values at 10 L/min are 0.77, 0.89, 1.00, and 1.07 at (%wt 0.0, 0.1, 0.2, and 0.3) volumetric concentrations, respectively.

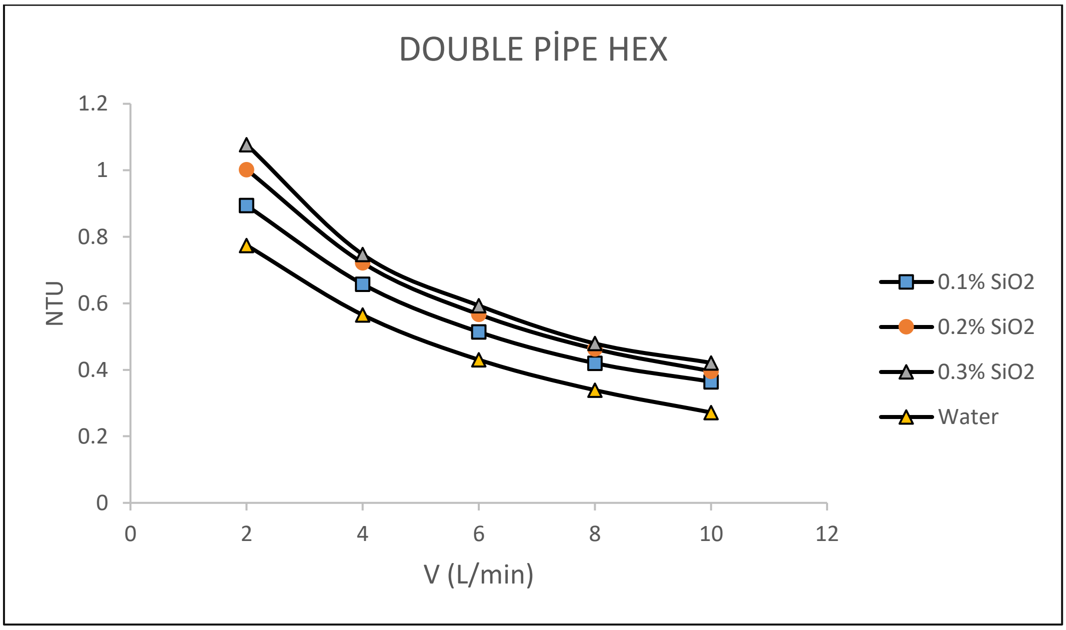

Figure 4.5 Volumetric rate and NTU results for double pipe heat exchanger

In figure 4.6 for the plate heat exchanger, five volumetric flow rates of (2, 4, 6, 8, and 10) liters/min are used. Three volumetric concentrations of SiO_2 nanofluid are used. (%wt 0.1, 0.2, and 0.3). It is noticed from the figure that the NTU values reduce when the fluid flow rate increases and the volumetric concentration rises of SiO_2 in the water, the more its NTU values of it increase successively. Whereas the NTU values at 10 L/min are 1.07, 1.36, 1.48, and 1.59 at (%wt 0.0, 0.1, 0.2, and 0.3) volumetric concentrations, respectively.

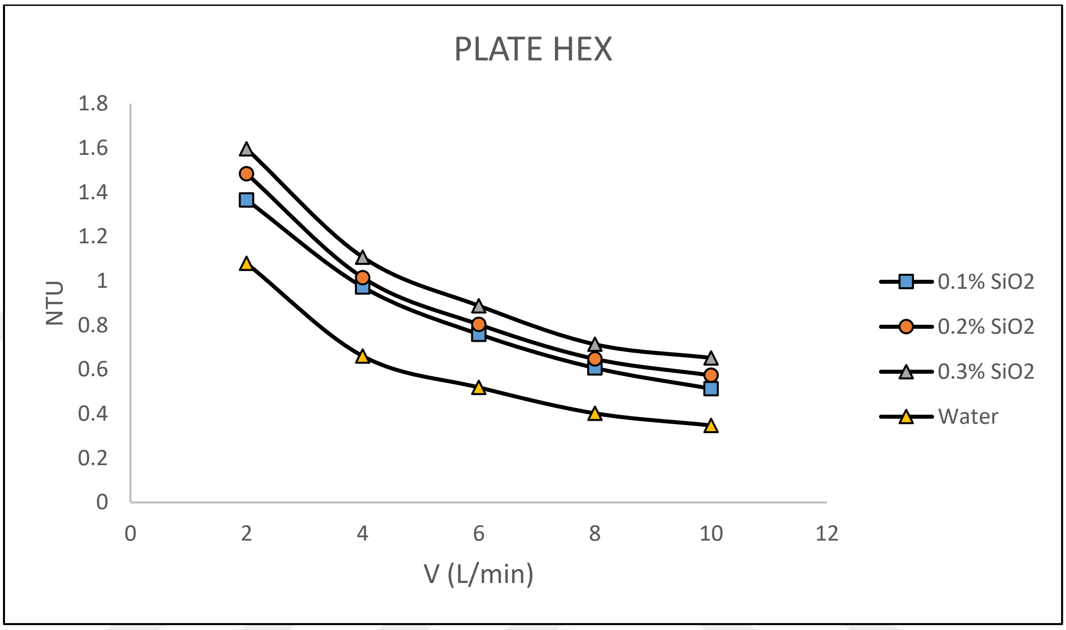

Figure 4.6 Volumetric rate and NTU results for plate heat exchanger

When examining Figure 4.4 and Figure 4.5, and Figure 4.6, it is noted that the highest rates of improvement in NTU appeared in the plate heat exchanger, followed by the double pipe heat exchanger, and the last one being the STHE.

4.3 Entropy Generation Results

The main objective of the study is to reduce entropy generation using SiO_2/water nanofluid; three volumetric concentrations of the fluid were used in Figure 4.7, and for the STHE at volume flow values of (2, 4, 6, 8, and 10) liters/min showing the percentages of entropy reduction compared to the liquid The main one which is water, we significantly improved the performance, at 0.1% SiO_2, and the volume flow values of (2, 4, 6, 8, and 10) liters/min the minimization ratios of entropy generation were (%wt 20.32, 22.54, 14.10, 17.09, 20.61), respectively. Moreover, at 0.2% SiO_2 and the volume flow values of (2, 4, 6, 8, and 10) liters/min, the minimization ratios of entropy generation were (%wt 34.68, 33.80, 27.68, 25.55, 29.40), respectively. Moreover, at 0.3% SiO_2 and the volume flow values of (2, 4, 6, 8, and 10) liters/min, the minimization ratios of entropy generation were (%wt 51.70, 48.89, 31.10, 33.49, 31.82), respectively.

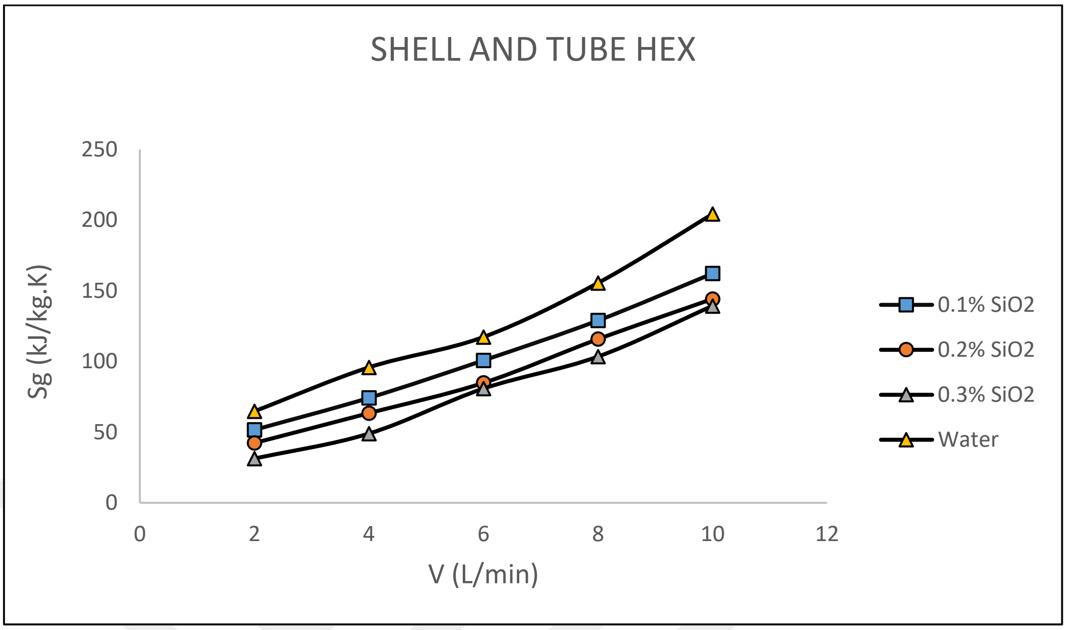

Figure 4.7 Volumetric rate and entropy generation results for shell and tube heat exchanger

In Figure 4.8 and for the DPHE at volume flow values of (2, 4, 6, 8, and 10) liters/min showing the percentages of entropy reduction compared to the liquid. For the main one, which is water, we significantly improved the performance; at 0.1% SiO_2 and the volume flow values of (2, 4, 6, 8, and 10) liters/min, the minimization ratios of entropy generation were (%wt 15.91, 6.44, 2.27, 3.34, 3.30), respectively. Moreover, at 0.2% SiO_2 and the volume flow values of (2, 4, 6, 8, and 10) liters/min, the minimization ratios of entropy generation were (%wt 26.56, 17.52, 7.87, 8.96, 6.71), respectively. Moreover, at 0.3% SiO_2 and the volume flow values of (2, 4, 6, 8, and 10) liters/min, the minimization ratios of entropy generation were (%wt 39.32, 26.92, 19.74, 14.35, 11.90), respectively. A clear improvement can be observed through the above ratios in reducing entropy generation for double-pipe heat exchangers.

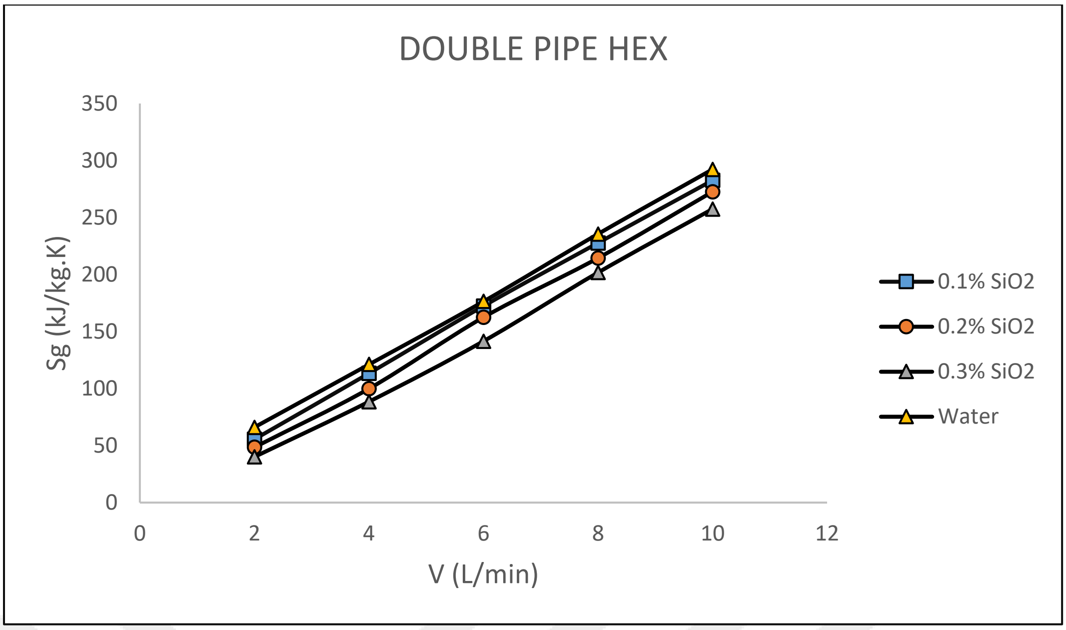

Figure 4.8 Volumetric rate and entropy generation results for DPHE

In Figure 4.9 and for the plate heat exchanger at volume flow values of (2, 4, 6, 8, and 10) liters/min showing the percentages of entropy reduction compared to the liquid. For the main one, which is water, we significantly improved the performance; at 0.1% SiO_2 and the volume flow values of (2, 4, 6, 8, and 10) liters/min, the minimization" ratios of entropy generation were (%wt 30.17, 22.54, 17.85, 16.54, 10.72), respectively. Moreover, at 0.2% SiO_2 and the volume flow values of (2, 4, 6, 8, and 10) liters/min, the minimization ratios of entropy generation were (%wt 54.87, 44.24, 32.95, 28.11, 21.40), respectively. Moreover, at 0.3% SiO_2 and the volume flow values of (2, 4, 6, 8, and 10) liters/min, the minimization ratios of entropy generation were (%wt 56.50, 52.47, 45.72, 39.51, 34.48, 11.90), respectively. A clear improvement can be observed through the above ratios in reducing entropy generation for double-pipe heat exchangers.

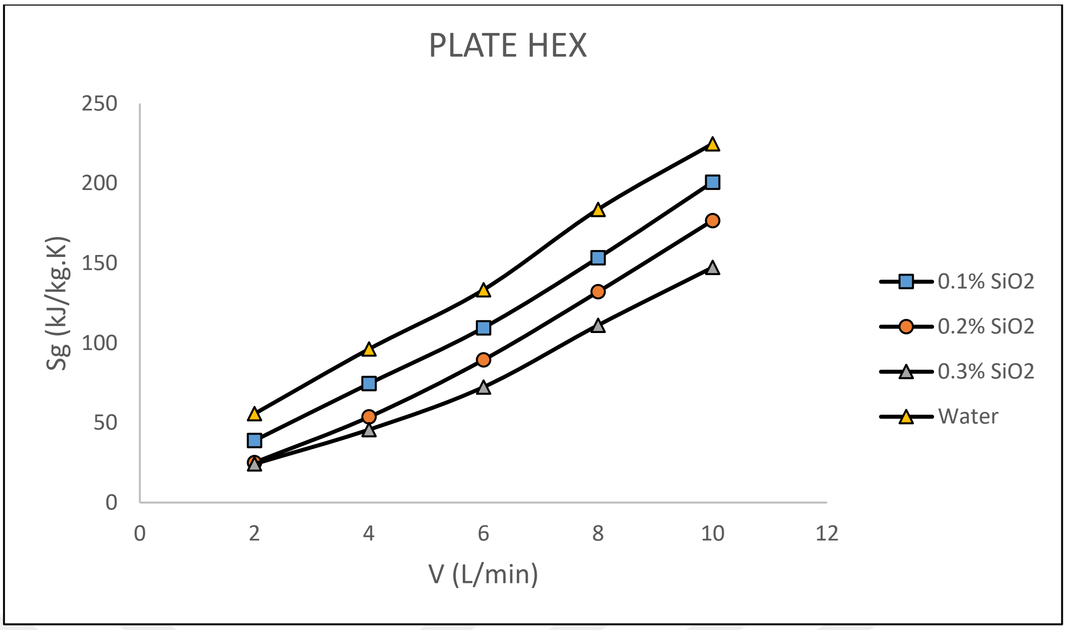

Figure 4.9 Volumetric rate and entropy generation results for plate heat exchanger

When we examine Figure 4.10, Figure 4.11, and Figure 4.12, which show the NTU values and compare them with the entropy values, it is noticed that when the volumetric flow rate increases, the NTU value decreases, and the entropy increases. In addition, when the volumetric concentration of the nanofluid is increased, the NTU value increases significantly, and the entropy generation decreases, which is consistent with the laws of thermodynamics. It is noted that the entropy generation values were at the double pipe heat exchanger and the lowest at the shell and tube heat exchanger. Also, the highest values of NTU were at the plate heat exchanger and the lowest at the shell and tube heat exchanger.

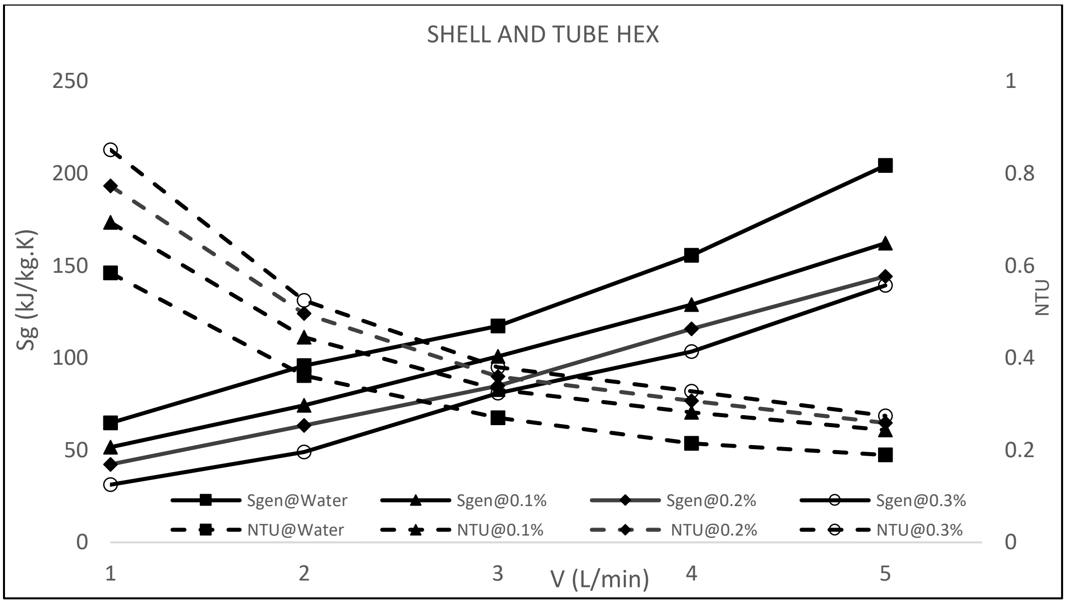

Figure 4.10 NTU and entropy generation results with volumetric rate for shell and tube heat exchanger

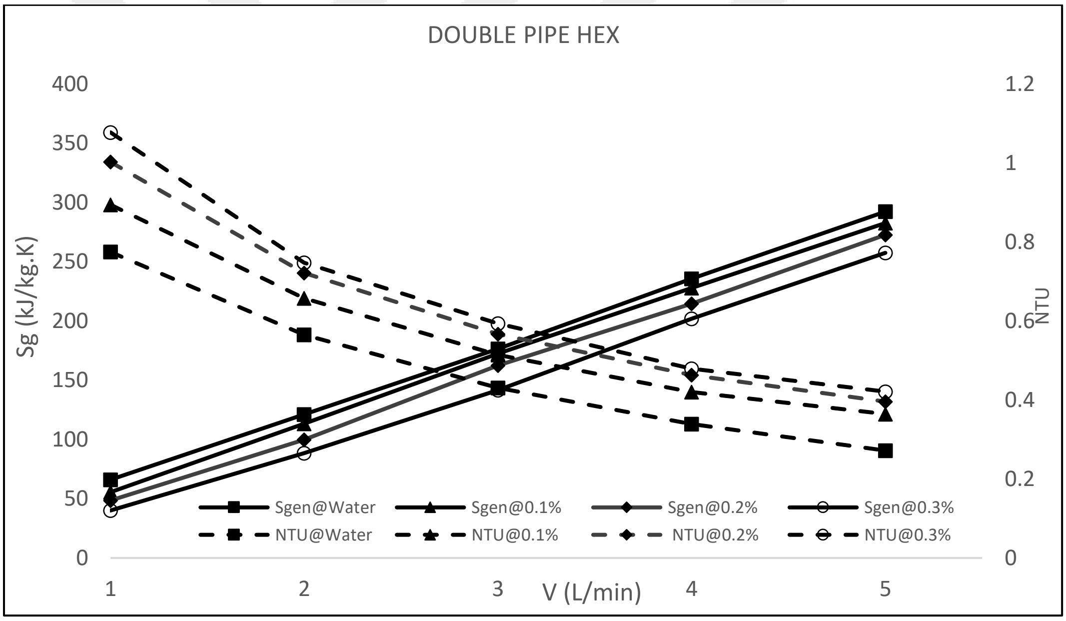

Figure 4.11 NTU and entropy generation results with volumetric rate for double pipe heat exchanger

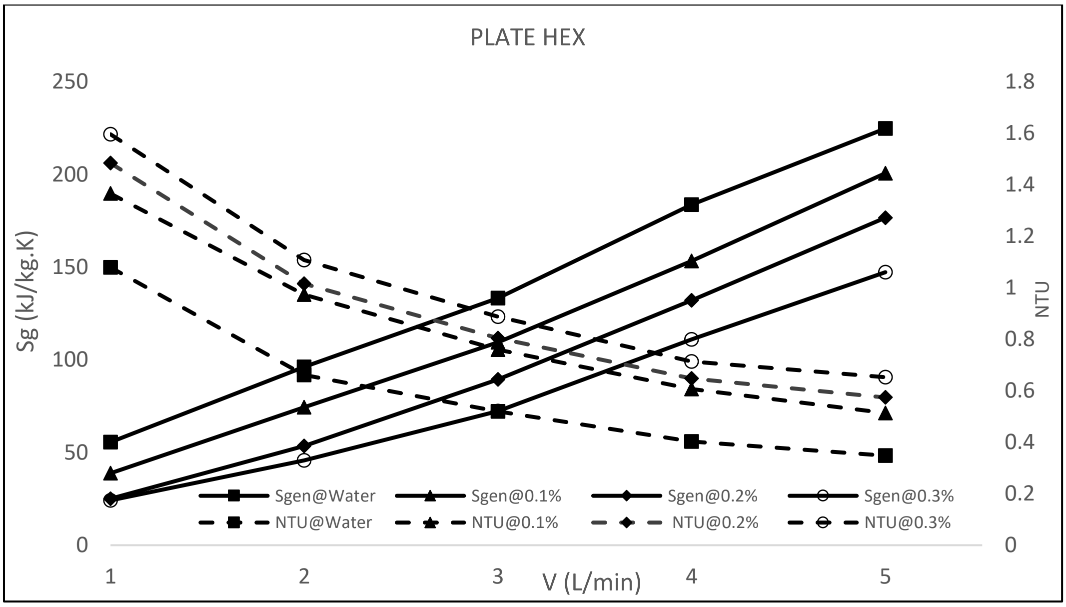

Figure 4.12 NTU and entropy generation results with volumetric rate for plate heat exchanger

Table 4.1 Inputs and outputs of experiment

INPUTS		OUTPUTS								
Ø	V L/min	STHE			DPHE			PHE		
		$\dot{S}g$	E	NTU	$\dot{S}g$	ε	NTU	$\dot{S}g$	ε	NTU
0	2	64.76	0.4199	0.5844	66.03	0.4898	0.7745	55.60	0.5901	1.0792
	4	95.83	0.2782	0.3618	121.11	0.3847	0.5651	96.15	0.3957	0.6609
	6	117.33	0.2142	0.2699	176.37	0.3045	0.4303	133.30	0.3373	0.5192
	8	155.58	0.1737	0.2146	235.57	0.2466	0.3390	183.65	0.2803	0.4024
	10	204.37	0.1543	0.1894	292.24	0.2012	0.2719	224.80	0.2492	0.3479
0.1	2	51.60	0.4511	0.6941	55.52	0.5432	0.8940	38.82	0.6521	1.3657
	4	74.22	0.3222	0.4450	113.30	0.4206	0.6576	74.47	0.5168	0.9731
	6	100.78	0.2489	0.3309	172.35	0.3424	0.5139	109.50	0.4348	0.7599
	8	128.99	0.2143	0.2819	227.70	0.2882	0.4201	153.27	0.3658	0.6073
	10	162.24	0.1873	0.2435	282.59	0.2532	0.3644	200.70	0.3183	0.5136
0.2	2	42.29	0.5100	0.7731	48.49	0.5853	1.0022	25.09	0.6863	1.4841
	4	63.43	0.3490	0.4965	99.89	0.4497	0.7216	53.60	0.5328	1.0152
	6	84.84	0.2669	0.3598	162.49	0.3650	0.5669	89.37	0.4485	0.8038
	8	115.82	0.2299	0.3070	214.45	0.3078	0.4630	132.03	0.3801	0.6478
	10	144.27	0.1973	0.2592	272.63	0.2683	0.3958	176.68	0.3408	0.5738
0.3	2	31.27	0.5300	0.8516	40.07	0.6171	1.0773	24.18	0.7057	1.5962
	4	48.98	0.3653	0.5248	88.50	0.4566	0.7472	45.70	0.5622	1.1077
	6	80.84	0.2778	0.3796	141.54	0.3757	0.5932	72.36	0.4756	0.8881
	8	103.47	0.2410	0.3281	201.76	0.3150	0.4793	111.09	0.4013	0.7138
	10	139.34	0.2059	0.2745	257.46	0.2799	0.4212	147.28	0.3667	0.6526

4.4 Response Surface Method

Models of efficiency and reduce the generation of entropy and heat transfer units were developed using experiments in addition to calculating error rates by RSM (Table 4.2), (Table 4.3), (Table 4.4), and when it was compared to the mathematical models, The error rate is indicated to be within an acceptable range.

The model's significance was determined using analysis of variance (ANOVA). Many model-related information are provided in the ANOVA tables. The table displays the average squares, standard deviation and variance, and degrees of freedom for the model. The tables illustrate the results of the data analysis (ANOVA table) of the linear regression used to define the efficacy, heat transfer units, and entropy of the heat exchangers. It is highlighted in Table 4.2's effectiveness findings that the model created for the efficiency calculations has an F-value of 492,59 and a p-value of less than (0.05). These findings show that the model is trustworthy and applicable to further analysis and optimization issues. Table 4.3 shows that the model created for NTU calculations has an F-value of 339,66 and a P-value of 0.05. Table 4.4 shows that the model created for entropy generation calculations has an F-value of 1076,77 and a P-value of 0.05. These findings demonstrate the model's dependability and show that it may be used for other analysis and optimization issues. as demonstrated by the RSM model-based experimental strategy.

Table 4.2 ANOVA table for effectiveness (Ɛ).

Source	DF	Adj SS	Adj MS	F-Value	P-Value
Model	11	1,08816	0,098923	492,59	0,000
Linear	4	1,02200	0,255501	1272,28	0,000
Flow(lpm)	1	0,69097	0,690968	3440,70	0,000
Fluid concentration	1	0,07438	0,074384	370,40	0,000
Type	2	0,25665	0,128326	639,00	0,000
Square	2	0,05726	0,028629	142,56	0,000
Flow(lpm)*Flow(lpm)	1	0,05163	0,051627	257,08	0,000
Fluid concentration*Fluid concentration	1	0,00563	0,005631	28,04	0,000
2-Way Interaction	5	0,00890	0,001779	8,86	0,000
Flow(lpm)*Fluid concentration	1	0,00179	0,001794	8,93	0,004
Flow(lpm)*Type	2	0,00326	0,001632	8,13	0,001
Fluid concentration*Type	2	0,00384	0,001919	9,56	0,000
Error	48	0,00964	0,000201		
Total	59	1,09780			

Table 4.3 ANOVA table for number of transfer unit (NTU).

Source	DF	Adj SS	Adj MS	F-Value	P-Value
Model	11	5,73857	0,52169	339,66	0,000
Linear	4	5,12127	1,28032	833,59	0,000
Flow(lpm)	1	2,82411	2,82411	1838,73	0,000
Fluid concentration	1	0,45442	0,45442	295,86	0,000
Type	2	1,84274	0,92137	599,89	0,000
Square	2	0,32404	0,16202	105,49	0,000
Flow(lpm)*Flow(lpm)	1	0,29634	0,29634	192,94	0,000
Fluid concentration*Fluid concentration	1	0,02771	0,02771	18,04	0,000
2-Way Interaction	5	0,29326	0,05865	38,19	0,000
Flow(lpm)*Fluid concentration	1	0,03246	0,03246	21,13	0,000
Flow(lpm)*Type	2	0,18188	0,09094	59,21	0,000

Fluid concentration*Type	2	0,07892	0,03946	25,69	0,000
Error	48	0,07372	0,00154		
Total	59	5,81229			

Table 4.4 ANOVA table for entropy generation ($\boldsymbol{S_{gen}}$).

Source	**DF**	**Adj SS**	**Adj MS**	**F-Value**	**P-Value**
Model	11	284082	25826	1076,77	0,000
Linear	4	266098	66525	2773,65	0,000
Flow(lpm)	1	200892	200892	8375,93	0,000
Fluid concentration	1	17442	17442	727,23	0,000
Type	2	47764	23882	995,72	0,000
Square	2	574	287	11,96	0,000
Flow(lpm)*Flow(lpm)	1	453	453	18,89	0,000
Fluid concentration*Fluid concentration	1	121	121	5,03	0,030
2-Way Interaction	5	17411	3482	145,18	0,000
Flow(lpm)*Fluid concentration	1	706	706	29,44	0,000
Flow(lpm)*Type	2	15740	7870	328,12	0,000
Fluid concentration*Type	2	965	483	20,12	0,000
Error	48	1151	24		
Total	59	285234			

The statistical analyses in the Figures, including the analysis of variance, were produced using Minitab 19 software (ANOVA). Figures 4.13, 4.14, and 4.15 demonstrate a decent agreement between the residuals' normality graphs.“ When the Entropy generation, NTU, and Epsilon distribution graphs are evaluated, the results are symmetric and extremely near to the normal distribution. Normally distributed diagrams show that sites with zero residuals have more data density.”It can be observed that these values all values stay between -1 and 1; this makes the model more trustworthy. The residuals' random distribution around the "0" line demonstrates the accuracy of the linearity assumption. When the resulting graphs are assessed generally, it shows that the model developed is trustworthy and the findings obtained are consistent.

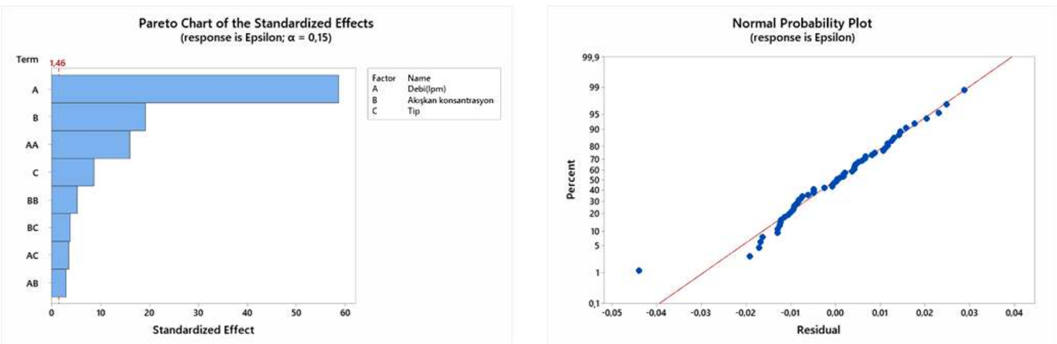

(a) (b)

Figure 4. 13 (a) Paretoichart for Ɛ; (b) Normal Probability plot for Ɛ

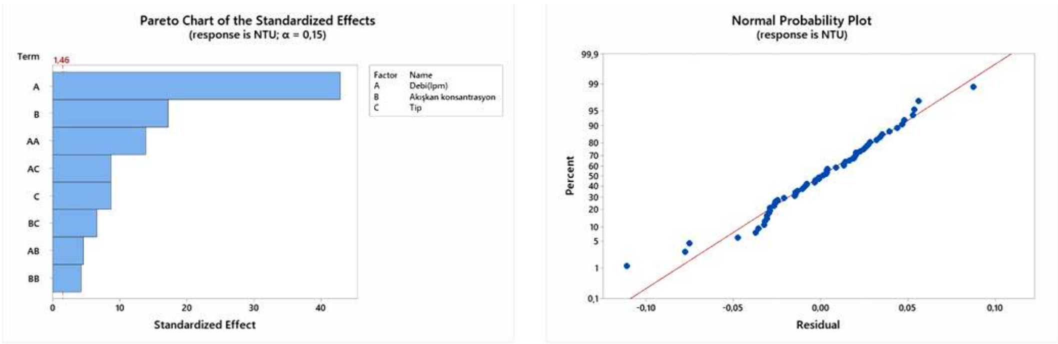

(a) (b)

Figure 4. 14 (a) Pareto chart for NTU; (b) Normal Probability plot for NTU

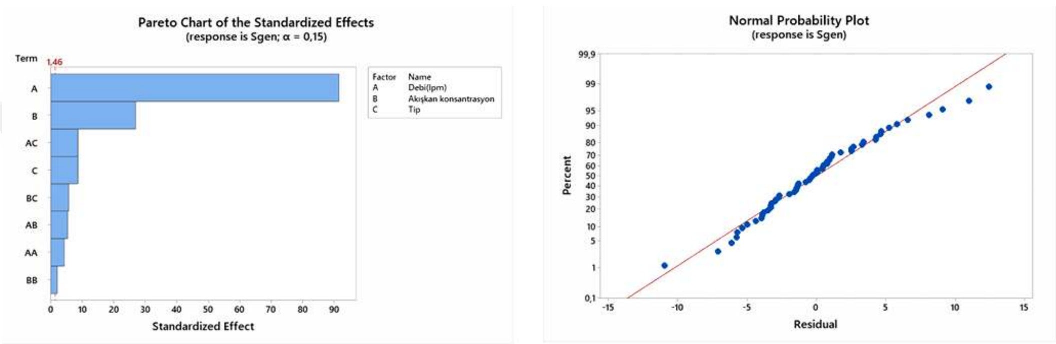

(a) (b)

Figure 4. 15 (a) Sgen Pareto chart; (b) Sgen Normal Probability Plot

Figures 4.16, 4.17, and 4.18 included a variance analysis (ANOVA). The standard graphs of the residual values are in good agreement; it may be claimed. Examining the produced histograms reveals that the data is symmetric and closely resembles a normal distribution. The locations where the residues are 0 are where the data is denser, as seen by an examination of the typical probability plots. The histogram in Figures 4.16, 4.17 and 4.18 of the effectiveness, NTU and S_{gen} study shows that the highest frequency values are near zero or very close to zero. The versus order chart also shows that the values are distributed positively and negatively in a waveform around zero areas. This arrangement shows that the analysis is highly acceptable and is like a typical histogram.

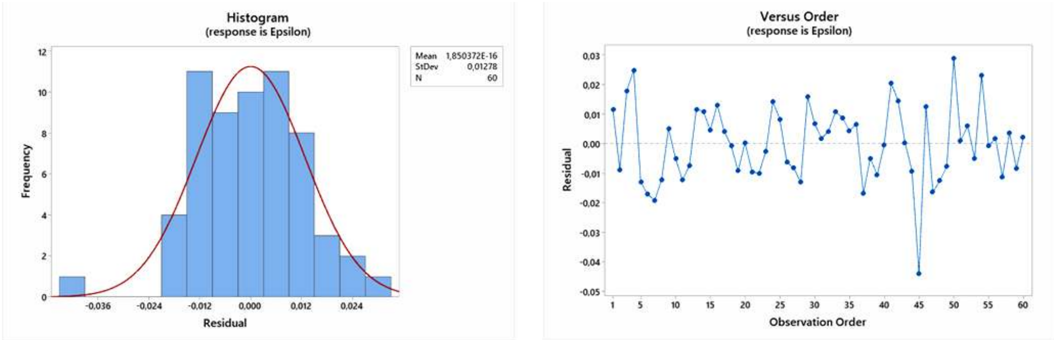

(a) (b)

Figure 4. 16 (a) Histogram for effectiveness (Ɛ); (b) versus order for effectiveness (Ɛ)

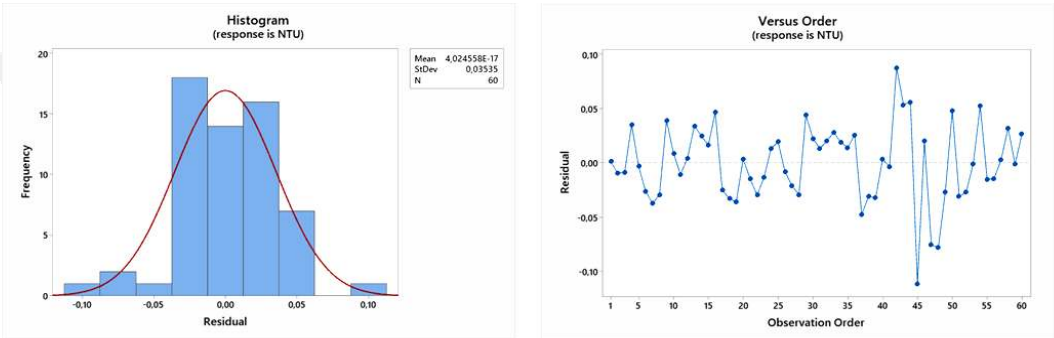

(a) (b)

Figure 4. 17 (a) Histogram for NTU; (b) versus order for NTU

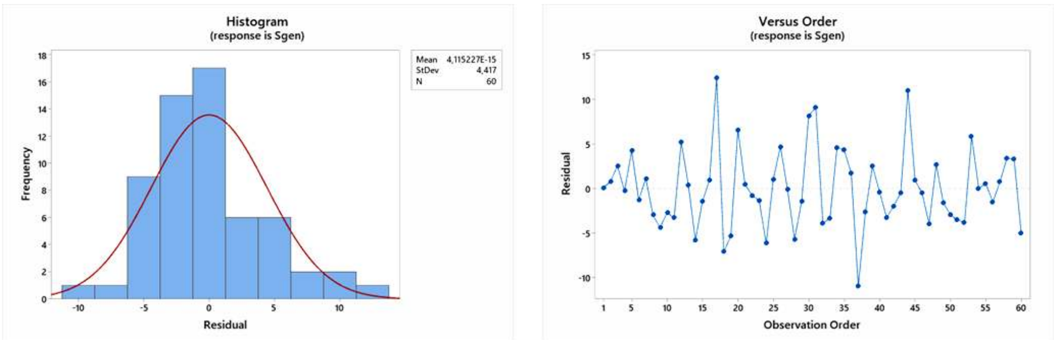

(a) (b)

Figure 4. 18 (a) Histogram for entropy generation (S_{gen}), (b) versus order for entropy generation (S_{gen})

5. CONCLUSIONS AND DISCUSSION

In this study, some variables such as volumetric flow rate, temperature, and volumetric concentration of the nanofluid in the heat exchangers were studied. Different heat exchangers are used (plate, shell and tube and double pipe) heat exchangers. The parameters were studied and analyzed by three methods, namely, entropy generation minimazation method, ε- NTU method and RSM method. The SiO_2/water nanofluid was used as a coolant, the volumetric concentrations of the nanofluid were determined at four concentrations (%wt 0.0, 0.1, 0.2, 0.3).

- The addition of nanofluids to the shell and tube heat exchanger with a volumetric concentration of 0.1% of SiO_2 nanoparticles reduced the entropy generation by 22.54% and when the volumetric concentration was increased to 0.2% the entropy generation was 33.80% and at 0.3% it was 48.89%. Increasing the amount of SiO_2 to the water used as a coolant reduces entropy generation and improves the performance of the shell and tube heat exchanger.
- As for the double pipe heat exchanger and for the same conditions in terms of volumetric concentration and temperature, at 0.1% the entropy generation percentage was 15.91%, at 0.2% it was 17.52%, and at 0.3% it was 39.32%, and it conclude that the generation of entropy decreases by increasing the volumetric concentration of the nanofluid.
- In the plate heat exchanger with 0.1% SiO_2/water, the addition of the nanofluid reduced the entropy generation by 30.17%, 54.87% at 0.2% SiO_2/water and 56.50% at 0.3% SiO_2/water, which is a decrease in entropy generation due to an increase in volumetric concentration of nanofluid.
- SiO_2 nanoparticles improve the work of the heat exchanger due to their effectiveness in increasing the thermal conductivity and the number of heat transfer units (NTU), that increasing the volumetric concentration of the nanofluid leads to an increase in the surface area, which in turn leads to an increase in thermal conductivity.
- The effectiveness was increased by 25.98% and 39.06% at 0.3% SiO_2 for the double tube heat exchanger. At the nanofluid volume 2 Liters/min and 10 Liters/min flow rates over the base fluid, respectively, the effectiveness

of the plate heat exchanger was increased by 19.58% and 47.08% over the base fluid. In addition, the shell and tube heat exchanger's effectiveness are improved. by 26.21% and 33.39%, respectively, with nanofluid volume 2 liters/min and 10 liters/min flow rates over the base fluid. It has been shown that the effectiveness of the nanofluid improves with increasing concentration of volume and decreases with volume flow rate."

- Shell and tube heat exchanger, the NTU values at 10 L/min are 0.58, 0.69, 0.77, and 0.85 at volumetric concentrations of 0.0% 0.1%, 0.2%, and 0.3%, respectively, and in the double pipe heat exchanger the NTU values at 10 L/min are 0.77 and 0.89, 1.00 and 1.07 at volumetric concentrations of 0.0% 0.1%, 0.2% and 0.3%, respectively. For the plate heat exchanger, the NTU values at 10 L/min are 1.07, 1.36, 1.48 and 1.59 at volumetric concentrations of 0.00% 0.10% and 0.20% and 0.30%, respectively. It seems in all the results that SiO_2 nanoparticles contribute effectively to improving the work of heat exchangers and can have a significant role in developing and improving heat transfer and cooling processes in various fields.
- The statistical analyses, including the analysis of variance, were produced using Minitab 19 software (ANOVA). When the Entropy generation, NTU, and Epsilon distribution graphs are evaluated, the results are symmetric and very near to the normally distributed. The standard probability diagrams reveal that locations with zero residuals have denser data.
- The standard graphs of the residual values are in good agreement. Examining the produced histograms reveals that the data is symmetric and closely resembles a normal distribution. The locations where the residues are 0 are where the data is denser, as seen by an examination of the typical probability plots. The effectiveness, NTU, and sgen study's histograms show that the highest frequency values are near zero or very close to zero. The versus order chart also shows that the values are distributed positively and negatively in a waveform around zero areas. This arrangement shows that the analysis is highly acceptable and is like a typical histogram.

6. REFERENCES

"Vancouver citation system was used in this thesis."

1. Esfahani MR, Languri EM. Exergy analysis of a shell-and-tube heat exchanger using graphene oxide nanofluids. Exp Therm Fluid Sci. 2017; 83:100–6.

2. Devalapally H., Chakilam A. AMM. Role of nanotechnology in pharmaceutical product development, J Pharm Sci. 2007;96:2547–2565.

3. Choi S.U.S. Enhancing thermal conductivity of fluids with nanoparticles. Proc ASME Int Mech Eng Congress Expos. 1995; 66:99–105.

4. Koutahzadeh N., Esfahani M.R., Arce PE. Removal of acid black 1 from water by the pulsed corona discharge advanced oxidation method, J Water Process Eng. 10:1–8.

5. Yang R., Qin Y., Dai L. WZL. Power generation with laterally packaged piezoelectric fine wires, Nat Nanotechnol. 2009;(4):34–39.

6. Esfahani M.R., Tyler J.L., Stretz H.A. WMJ. Effects of a dual nanofiller, nano-TiO2 and MWCNT, for polysulfone-based nanocomposite membranes for water purification, Desalination. 372:47–56.

7. M.R. Esfahani, J.L. Tyler, H.A. Stretz, M.J. Wells. Effects of a dual nanofiller, nano-TiO2 and MWCNT, for polysulfone-based nanocomposite membranes for water purification, Desalination. 372:47–56.

8. Lomascolo M., Colangelo G., Milanese M. de RA. Review of heat transfer in nanofluids: conductive, convective and radiative experimental results, Rev. Renew Sustain Energy. 43:1182–1198.

9. Julia JE, Hernández L, Martínez-Cuenca R, Hibiki T, Mondragón R, Segarra C, et al. Measurement and modelling of forced convective heat transfer coefficient and pressure drop of Al2O3- and SiO2-water nanofluids. J Phys Conf Ser. 2012;395(1).

10. Kulkarni DP, Namburu PK, Ed Bargar H, Das DK. Convective heat transfer and fluid dynamic characteristics of SiO 2 - Ethylene glycol/water nanofluid. Heat Transfer Engineering. 2008 Dec;29(12):1027–35.

11. Darzi AAR, Farhadi M, Sedighi K, Shafaghat R, Zabihi K. Experimental investigation of turbulent heat transfer and flow characteristics of SiO 2/water nanofluid within helically corrugated tubes. International Communications in Heat and Mass Transfer. 2012;39(9):1425–34.

12. Jafarzad A, Heyhat MM. Thermal and exergy analysis of air- nanofluid bubbly flow in a double-pipe heat exchanger. Powder Technol. 2020; 372:563–77.

13. Huminic G, Huminic A. Application of nanofluids in heat exchangers: A review. Renewable and Sustainable Energy Reviews. 2012;16(8):5625–38.

14. Bellahcene L, Sahel D, Yousfi A. Numerical Study of Shell and Tube Heat Exchanger Performance Enhancement Using Nanofluids and Baffling Technique. Journal of Advanced Research in Fluid Mechanics and Thermal Sciences. 2021;80(2):42–55.

15. Maddah H, Ghasemi N, Keyvani B, Cheraghali R. Experimental and numerical study of nanofluid in heat exchanger fitted by modified twisted tape: exergy analysis and ANN prediction model. Heat and Mass Transfer/Waerme- und Stoffuebertragung. 2017;53(4):1413–23.

16. Qi C, Liu M, Wang G, Pan Y, Liang L. Experimental research on stabilities, thermophysical properties and heat transfer enhancement of nanofluids in heat exchanger systems. Chin J

Chem Eng. 2018;26(12):2420–30.

17. Khedkar RS, Sonawane SS, Wasewar KL. Water to nanofluids heat transfer in concentric tube heat exchanger: Experimental study. Procedia Eng. 2013; 51:318–23.

18. Farajollahi B, Etemad SG, Hojjat M. Heat transfer of nanofluids in a shell and tube heat exchanger. Int J Heat Mass Transf. 2010;53(1–3):12–7.

19. Arsana IM, Agista DR, Ansori A, Sutjahjo DH, Effendy M. The Effect of Nanofluid Volume Fraction to the Rate of Heat Transfer Convection Nanofluid Water-Al2O3 on Shell and Tube Heat Exchanger. In: Journal of Physics: Conference Series. 2020. p. 0–6.

20. Almurtaji S, Ali N, Teixeira JA, Addali A. On the role of nanofluids in thermal-hydraulic performance of heat exchangers-a review. Nanomaterials. 2020;10(4).

21. Albadr J, Tayal S, Alasadi M. Heat transfer through heat exchanger using Al2O3 nanofluid at different concentrations. Case Studies in Thermal Engineering. 2013;1(1):38–44.

22. Fard MH, Talaie MR, Nasr S. Numerical and experimental investigation of heat transfer of zno/water nanofluid in the concentric tube and plate heat exchangers. Thermal Science. 2011;15(1):183–94.

23. Jalili B, Aghaee N, Jalili P, Domiri Ganji D. Novel usage of the curved rectangular fin on the heat transfer of a double-pipe heat exchanger with a nanofluid. Case Studies in Thermal Engineering. 2022 Jul; 35:102086.

24. Qi C, Luo T, Liu M, Fan F, Yan Y. Experimental study on the flow and heat transfer characteristics of nanofluids in double-tube heat exchangers based on thermal efficiency assessment. Energy Convers Manag. 2019;197(May):111877.

25. Vahdat Azad A, Vahdat Azad N. Application of nanofluids for the optimal design of shell and tube heat exchangers using genetic algorithm. Case Studies in Thermal Engineering. 2016; 8:198–206.

26. Huang D, Wu Z, Sunden B. Effects of hybrid nanofluid mixture in plate heat exchangers. Experimental Thermal and Fluid Science. 2016; 72:190–6.

27. Jafarzad A, Heyhat MM. Thermal and exergy analysis of air- nanofluid bubbly flow in a double-pipe heat exchanger. Powder Technol. 2020; 372:563–77.

28. Huminic G, Huminic A. Application of nanofluids in heat exchangers: A review. Renewable and Sustainable Energy Reviews. 2012;16(8):5625–38.

29. Bellahcene L, Sahel D, Yousfi A. Numerical Study of Shell and Tube Heat Exchanger Performance Enhancement Using Nanofluids and Baffling Technique. Journal of Advanced Research in Fluid Mechanics and Thermal Sciences. 2021;80(2):42–55.

30. Maddah H, Ghasemi N, Keyvani B, Cheraghali R. Experimental and numerical study of nanofluid in heat exchanger fitted by modified twisted tape: exergy analysis and ANN prediction model. Heat and Mass Transfer/Waerme- und Stoffuebertragung. 2017;53(4):1413–23.

31. Qi C, Liu M, Wang G, Pan Y, Liang L. Experimental research on stabilities, thermophysical properties and heat transfer enhancement of nanofluids in heat exchanger systems. Chin J Chem Eng. 2018;26(12):2420–30.

32. Khedkar RS, Sonawane SS, Wasewar KL. Water to nanofluids heat transfer in concentric tube heat exchanger: Experimental study. Procedia Eng. 2013; 51:318–23.

33. Farajollahi B, Etemad SG, Hojjat M. Heat transfer of nanofluids in a shell and tube heat exchanger. Int J Heat Mass Transf. 2010;53(1–3):12–7.

34. Arsana IM, Agista DR, Ansori A, Sutjahjo DH, Effendy M. The Effect of Nanofluid Volume

Fraction to the Rate of Heat Transfer Convection Nanofluid Water-Al2O3 on Shell and Tube Heat Exchanger. In: Journal of Physics: Conference Series. 2020. p. 0–6.

35. Almurtaji S, Ali N, Teixeira JA, Addali A. On the role of nanofluids in thermal-hydraulic performance of heat exchangers-a review. Nanomaterials. 2020;10(4).

36. Albadr J, Tayal S, Alasadi M. Heat transfer through heat exchanger using Al2O3 nanofluid at different concentrations. Case Studies in Thermal Engineering. 2013;1(1):38–44.

37. Fard MH, Talaie MR, Nasr S. Numerical and experimental investigation of heat transfer of zno/water nanofluid in the concentric tube and plate heat exchangers. Thermal Science. 2011;15(1):183–94.

38. Qi C, Luo T, Liu M, Fan F, Yan Y. Experimental study on the flow and heat transfer characteristics of nanofluids in double-tube heat exchangers based on thermal efficiency assessment. Energy Convers Manag. 2019;197(May):111877.

39. Vahdat Azad A, Vahdat Azad N. Application of nanofluids for the optimal design of shell and tube heat exchangers using genetic algorithm. Case Studies in Thermal Engineering. 2016; 8:198–206.

40. Bashtani I, Esfahani JA. ε-NTU analysis of turbulent flow in a corrugated double pipe heat exchanger: A numerical investigation. Appl Therm Eng. 2019;159(May):1–11.

41. Dittus, F. and Boelter L. Heat transfer in automobile radiators of the tubular type. University of California Publications in Engineering. 1930;(2):443– 461.

42. S.U.S. Choi. Enhancing thermal conductivity of fluids with nanoparticles. Proc ASME Int Mech Eng Congress Expos. 1995; 66:99–105.

43. Keblinski, P., Eastman, J. A., and Cahill DG. Nanofluids for thermal transport. Materials Today, :36–44.

44. Pak, B. and Cho Y. Hydrodynamic and heat transfer study of dispersed fluids with submicron metallic oxide particles. Experimental Heat Transfer. 1998;11(2):151–170.

45. Das, S. K., Putta, N., Thiesen, P., and Roetzel W. Temperature dependence of thermal conductivity enhancement for nanofluids. ASME Trans J Heat Transfer. 125:567–574.

46. Xuan, Y. and Li Q. Investigation on convective heat transfer and flow features of nanofluids. J Heat Transfer. 2003; 125:151–155.

47. Yang, Y., Zhang, Z. G., Grulke, E. A. A, W. B., and Wu G. Heat transfer properties of nanoparticle-in-fluid dispersions (nanofluids) in laminar flow. Int J Heat Mass Transf. 2005;48(6):1107–1116.

48. Buongiorno J. Convective transport in nanofluids. J Heat Transfer. 2006; 128:240–250.

49. Polidori, G., Fohanno, S., and Nguyen CT. A note on heat transfer modelling of Newtonian nanofluids in laminar free convection. International Journal of Thermal Sciences. 2007;46(8):739–744.

50. Polidori, G., Fohanno, S., and Nguyen CT. A note on heat transfer modelling of Newtonian nanofluids in laminar free convection. International Journal of Thermal Sciences. 2007;46(8):739–744.

51. Gnielinski V. New equations for heat and mass transfer in turbulent pipe and channel flow. International Chemical Engineering. 1976;(16):359–368.

52. Mahian O, Kolsi L, Amani M, Estellé P, Ahmadi G, Kleinstreuer C, et al. Recent advances in modeling and simulation of nanofluid flows — Part I : Fundamentals and theory. Phys Rep. 2019; 790:1–48.

53. Tzeng, S.C., Lin, C.W. & Huang KD. Heat transfer enhancement of nanofluids in rotary blade coupling of four-wheel-drive vehicles. Acta Mech. 2005; 179:11–23.

54. Popa I, Gillies G, Papastavrou G BM. Attractive and repulsive electrostatic forces between positively charged latex particles in the presence of anionic linear polyelectrolytes. J Phys Chem B. 2010;114(3):170–3177.

55. Kao MJ, Lo CH, Tsung TT, Wu YY, Jwo CS LHM. Producing Aluminum-oxide brake nanofluids derived using plasma charging system. J Chin Soc Mech Eng. 2007; 28:123–31.

56. Shanthi R, Anandan Shanmuga Sundaram VR. Heat Transfer Enhancement Using Nanofluids- An Overview. Therm Sci. 2012;16(2):423–440.

57. Wei Yu Huaqing Xie A. Review on nanofluids: preparation, stability mechanisms and applications. J Nanomater. 2012;1–17.

58. Zhang L, Jiang Y, Ding Y, Povey M YD. Investigation into the antibacterial behaviour of suspensions of ZnO nanoparticles (ZnO nanofluids). J Nanopart Res. 2007;9(3):479–89.

59. Jalal R, Goharshadi EK, Abareshi M, Moosavi M, Yousefi A, Nancarrow P. ZnO nanofluids: green synthesis, characterization, and antibacterial activity. Materials Chemistry and Physics. 2010;121(1–2):198–201.

60. Panacek A, Kvitek L, Prucek R, Kolar M, Vecerova R, Pizurova N et al. silver colloid nanoparticles: synthesis, characterization, and their antibacterial activity. J Phys Chem B. 2006;110(33):16248–53.

61. Lyon DY APJJ. Fullerene water suspension (nC60) exerts antibacterial effects via ROS-independent protein oxidation. Environ Sci Technol. 2008;42(21):8127–32.

62. Asirvatham LG, Raja B, Mohan Lal D, Wongwises S. Convective heat transfer of nanofluids with correlations. Particuology. 2011;9(6):626–31.

63. Namburu PK, Das DK, Tanguturi KM, Vajjha RS. Numerical study of turbulent flow and heat transfer characteristics of nanofluids considering variable properties. International Journal of Thermal Sciences. 2009;48(2):290–302.

64. Ahammed N, Asirvatham LG, Wongwises S. Entropy generation analysis of graphene–alumina hybrid nanofluid in multiport minichannel heat exchanger coupled with thermoelectric cooler. International Journal of Heat and Mass Transfer. 2016; 103:1084–97.

65. Leong KY, Saidur R, Mahlia TMI, Yau YH. Modeling of shell and tube heat recovery exchanger operated with nanofluid based coolants. Int J Heat Mass Transf. 2012;55(4):808–16.

66. Zeinali Heris S, Nassan TH, Noie SH, Sardarabadi H, Sardarabadi M. Laminar convective heat transfer of Al2O3/water nanofluid through square cross-sectional duct. Int J Heat Fluid Flow. 2013; 44:375–82.

67. Naphon P, Nakharintr L. Heat transfer of nanofluids in the mini-rectangular fin heat sinks. International Communications in Heat and Mass Transfer. 2013;40(1):25–31.

68. Khairul MA, Saidur R, Rahman MM, Alim MA, Hossain A, Abdin Z. Heat transfer and thermodynamic analyses of a helically coiled heat exchanger using different types of nanofluids. Int J Heat Mass Transf. 2013; 67:398–403.

69. Zhang H, Gu C lin, Gu L wen, Zhang Y. The evaluation of tourism destination competitiveness by TOPSIS & information entropy - A case in the Yangtze River Delta of China. Tour Manag. 2011;32(2):443–51.

70. Patil, Sandesh & Sahu S. Thermal performance of Automobile Radiator Using CNT-water Nanofluid -Experimental Study. ASME - Journal of Thermal Science and Engineering Applications. 2014;(10.1115/1.4027678.).

71. Zamzamian A, Oskouie SN, Doosthoseini A, Joneidi A, Pazouki M. Experimental investigation of forced convective heat transfer coefficient in nanofluids of Al2O3/EG and CuO/EG in a double pipe and plate heat exchangers under turbulent flow. Exp Therm Fluid Sci. 2011;35(3):495–502.

72. Chen YJ, Wang PY, Liu ZH, Li YY. Heat transfer characteristics of a new type of copper wire-bonded flat heat pipe using nanofluids. Int J Heat Mass Transf. 2013; 67:548–59.

73. Lin CY, Wang JC, Chen TC. Analysis of suspension and heat transfer characteristics of Al2O3 nanofluids prepared through ultrasonic vibration. Appl Energy. 2011;88(12):4527–33.

74. Haghighi EB, Saleemi M, Nikkam N, Anwar Z, Lumbreras I, Behi M, et al. Cooling performance of nanofluids in a small diameter tube. Exp Therm Fluid Sci. 2013; 49:114–22.

75. Sharma S, Tiwari AK, Tiwari S, Prakash R. Viscosity of hybrid nanofluids: Measurement and comparison. Journal of Mechanical Engineering and Sciences. 2018;12(2):3614–23.

76. Suresh S, Chandrasekar M, Chandra Sekhar S. Experimental studies on heat transfer and friction factor characteristics of CuO/water nanofluid under turbulent flow in a helically dimpled tube. Exp Therm Fluid Sci. 2011;35(3):542–9.

77. Pantzali MN, Mouza AA, Paras S V. Investigating the efficacy of nanofluids as coolants in plate heat exchangers (PHE). Chem Eng Sci. 2009;64(14):3290–300.

78. Leong KY, Saidur R, Kazi SN, Mamun AH. Performance investigation of an automotive car radiator operated with nanofluid-based coolants (nanofluid as a coolant in a radiator). Appl Therm Eng. 2010;30(17–18):2685–92.

79. Pantzali MN, Mouza AA, Paras S V. Investigating the efficacy of nanofluids as coolants in plate heat exchangers (PHE). Chem Eng Sci. 2009;64(14):3290–300.

80. DAL AR. Düz Plakali Borulu Bi Değiştiricisinin Optimum Kanatçik Araliğinin SayisaAnalizi. Ömer Halisdemir Üniversitesi Mühendislik Bilimleri Dergisi. 2019;8(1):479–501.

81. Kırtepe E, Özbalta N. Kanatlı-borulu ısı değiştiricilerde belirsizlik analizi. Dicle Üniversitesi Mühendislik Fakültesi Mühendislik Dergisi. 2018;9(1):161–75.

82. Boran K, Daştan F, Şahin HM, Aktaş M. Isı Eşanjörlerinde Isı Transferi İyileştirme Yöntemlerinin Sayısal ve Deneysel Olarak İncelenmesi. Politeknik Dergisi. 2014;17(4):183–91.

83. Kizilkan Ö. Gövde Borulu Bir Isı Değiştiricisinde Şaşırtma Levhasının Isı Taşınım Katsayısına ve Basınç Düşümüne Etkisinin ncelenmesi. Fen Bilimleri Enstitüsü Dergisi. 2007;3(2007):246–51.

84. Abd AA, Naji SZ. Analysis study of shell and tube heat exchanger for clough company with reselect different parameters to improve the design. Case Studies in Thermal Engineering. 2017;10(October):455–67.

85. Akyürek EF, Geliş K, Yoladi M. Thermodynamic Analysis for Different Type of Heat Exchangers. Journal of the Institute of Science and Technology. 2020;10(2):1202–12.

86. Liu L, Ding N, Shi J, Xu N, Guo W, Wu CML. Failure analysis of tube-to-tubesheet welded joints in a shell-tube heat exchanger. Case Stud Eng Fail Anal. 2016; 7:32–40.

87. Mirzaei M, Hajabdollahi H, Fadakar H. Multi-objective optimization of shell-and-tube heat exchanger by constructal theory. Appl Therm Eng. 2017; 125:9–19.

88. Zhang, Xiang and Keramati, Hadi and Arie, Martinus and Singer, Farah and Tiwari, Ratnesh and Shooshtari, Amir and Ohadi M. Recent developments in high temperature heat

exchangers: A review. rontiers in Heat and Mass Transfer. 2018;11(10.5098/hmt.11.18).

89. Omidi M, Farhadi M, Jafari M. A comprehensive review on double pipe heat exchangers. Applied Thermal Engineering. 2017; 110:1075–90.

90. Liu SK& H. Heat Exchangers: Selection, Rating and Thermal Design CRC Press. 2005. ISBN 0-8493-0902-6.

91. Naphon P, Suchana T. Heat transfer enhancement and pressure drop of the horizontal concentric tube with twisted wires brush inserts. International Communications in Heat and Mass Transfer. 2011;38(2):236–41.

92. Ghani S, Gamaledin SMA, Rashwan MM, Atieh MA. Experimental investigation of double-pipe heat exchangers in air conditioning applications. Energy Build. 2018; 158:801–11.

93. Pourahmad S, Pesteei SM. Effectiveness-NTU analyses in a double tube heat exchanger equipped with wavy strip considering various angles. Energy Convers Manag. 2016; 123:462–9.

94. Gupta P, Atrey MD. Performance evaluation of counter flow heat exchangers considering the effect of heat in leak and longitudinal conduction for low-temperature applications. Cryogenics (Guildf). 2000;40(7):469–74.

95. https://empow-her.com/astro8be9/cbbce2274215.htm?p=5.1.145374.1.27.36.double+pipe+heat+exchanger.

96. Wang J. Pressure drop and flow distribution in parallel-channel configurations of fuel cells: U-type arrangement. Int J Hydrogen Energy. 2008;33(21):6339–50.

97. Zhou, J., Zhao, X., Ma, X., Du, Z., Fan, Y., Cheng, Y., Zhang, X. Clear-days operational performance of a hybrid experimental space heating system employing the novel mini-channel solar thermal & PV/T panels and a heat pump. Sol. Energy. 2017;155(https://doi.org/10.1016/J.SOLENER.2017.06.056.):464–477.

98. Rao RV, Patel V. Multi-objective optimization of heat exchangers using a modified teaching-learning-based optimization algorithm. Appl Math Model. 2013;37(3):1147–62.

99. Patel VK, Rao R V. Design optimization of shell-and-tube heat exchanger using particle swarm optimization technique. Appl Therm Eng. 2010;30(11–12):1417–25.

100. https://www.uappsweb.com/index.php?main_page=product_info&products_id=306974.

101. Zhou, J., Zhao, X., Ma, X., Du, Z., Fan, Y., Cheng, Y., Zhang, X. Clear-days operational performance of a hybrid experimental space heating system employing the novel mini-channel solar thermal & PV/T panels and a heat pump. Sol. Energy. 2017;155(https://doi.org/10.1016/J.SOLENER.2017.06.056.):464–477.

102. Zhang H, Gu C lin, Gu L wen, Zhang Y. The evaluation of tourism destination competitiveness by TOPSIS & information entropy - A case in the Yangtze River Delta of China. Tour Manag. 2011;32(2):443–51.

103. Teke I, Ağra Ö, Atayilmaz ŞÖ, Demir H. Determining the best type of heat exchangers for heat recovery. Appl Therm Eng. 2010;30(6–7):577–83.

104. Shirgire ND. Review on Comparative Study between Helical Coil and Straight Tube Heat Exchanger. IOSR Journal of Mechanical and Civil Engineering. 2013;8(2):55–9.

105. Ma W, Karbojian A, Sehgal BR, Dinh TN. Thermal-hydraulic performance of heavy liquid metal in straight-tube and U-tube heat exchangers. Nuclear Engineering and Design. 2009;239(7):1323–30.

106. Shirgire ND. Review on Comparative Study between Helical Coil and Straight Tube Heat

Exchanger. IOSR Journal of Mechanical and Civil Engineering. 2013;8(2):55–9.

107. Zhao Q, Liu F, Liu C, Tian M, Chen B. Influence of spiral pitch on the thermal behaviors of energy piles with spiral-tube heat exchanger. Appl Therm Eng. 2017;125(July 2017):1280–90.

108. Ardahaie SS, Hosseini MJ, Ranjbar AA, Rahimi M. Energy storage in latent heat storage of a solar thermal system using a novel flat spiral tube heat exchanger. Appl Therm Eng. 2019;159(April):113900.

109. https://www.alfalaval.com/products/heat-transfer/plate-heat-exchangers/welded-spiral-heat-exchangers/how-it-works/.

110. Mukherjee R. Effectively design hell-and-tube heat exchangers. Chem Eng Prog. 1998;94(2):21–37.

111. Wang S, Wen J, Li Y. An experimental investigation of heat transfer enhancement for a shell-and-tube heat exchanger. Appl Therm Eng. 2009;29(11–12):2433–8.

112. Abd AA, Kareem MQ, Naji SZ. Performance analysis of shell and tube heat exchanger: Parametric study. Case Studies in Thermal Engineering. 2018;12(December 2017):563–8.

113. Abbasian Arani AA, Moradi R. Shell and tube heat exchanger optimization using new baffle and tube configuration. Appl Therm Eng. 2019;157(January).

114. Abbasian Arani AA, Moradi R. Shell and tube heat exchanger optimization using new baffle and tube configuration. Appl Therm Eng. 2019;157(January).

115. Zheng, Dan & Wang, Jin & Chen, Zhanxiu & Baleta, Jakov & Sunden, Bengt. (2020). Performance analysis of a plate heat exchanger using various nanofluids. International Journal of Heat and Mass Transfer. 158. 119993. 10.1016/j.ijheatmasstransfer.2020.119993.

116. Andrey J, Gut W. Engineering Modeling of Plate Heat Exchangers with Generalized. 16th BRAZILIAN CONGRESS OF MECHANICAL. (1960).

117. Zheng, Dan & Wang, Jin & Chen, Zhanxiu & Baleta, Jakov & Sunden, Bengt. (2020). Performance analysis of a plate heat exchanger using various nanofluids. International Journal of Heat and Mass Transfer. 158. 119993. 10.1016/j.ijheatmasstransfer.2020.119993.

118. Akturk F, Sezer-uzol N, Aradag S, Kakac S, Savunma Sistemleri Ş FA, Mahallesi O, et al. Experimental Investigation and Performance Analysis of Gasketed-Plate Heat Exchangers. J of Thermal Science and Technology. 2015; 35:43–52.

119. Hajabdollahi H, Naderi M, Adimi S. A comparative study on the shell and tube and gasket-plate heat exchangers: The economic viewpoint. Appl Therm Eng. 2016; 92:271–82.

120. https://www.alfalaval.my/products/heat-transfer/plate-heat-exchangers/gasketed-plate-and-frame-heat-exchangers/heat-exchanger/how-plate-heat-exchanger-work/.

121. Rincón Tabares JS, Perdomo-Hurtado L, Aragón JL. Study of Gasketed-Plate Heat Exchanger performance based on energy efficiency indexes. Appl Therm Eng. 2019;159(May):113902.

122. Pradeep Mohan Kumar K, Vijayan V, Suresh Kumar B, Vivek CM, Dinesh S. Computational analysis and optimization of spiral plate heat exchanger. Journal of Applied Fluid Mechanics. 2018;11(Specialissue):121–8.

123. https://www.elancoheatexchangers.com/products/spiral-plate-heat-exchangers/.

124. Rajavel R. Experimental and numerical studies of a spiral plate heat exchanger. Thermal Science. 2014;18(4):1355–60.

125. Rajavel R, Saravanan K. Heat transfer studies on spiral plate heat exchanger. Thermal

Science. 2008;12(3):85–90.

126. Kumareswaran Subasgar. Shell and tube heat exchanger design for sulfuric acid manufacturing plant. 2014;(10.13140/RG.2.1.2721.6720/1.).

127. Kumareswaran Subasgar. Shell and tube heat exchanger design for sulfuric acid manufacturing plant. 2014;(10.13140/RG.2.1.2721.6720/1.).

128. Bhuiyan AA, Islam AKMS. Thermal and hydraulic performance of finned-tube heat exchangers under different flow ranges: A review on modeling and experiment. Int J Heat Mass Transf. 2016; 101:38–59.

129. Kim Y, Kim Y. Heat transfer characteristics of flat plate finned-tube heat exchangers with large fin pitch. International Journal of Refrigeration. 2005;28(6):851–8.

130. Kondepudi SN, O’Neal DL. Performance of finned-tube heat exchangers under frosting conditions: I. Simulation model. International Journal of Refrigeration. 1993;16(3):175–80.

131. https://www.enggcyclopedia.com/2012/03/finned-tube-heat-exchangers/.

132. Qian S, Yu J, Yan G. A review of regenerative heat exchange methods for various cooling technologies. Renewable and Sustainable Energy Reviews. 2017;69(October 2016):535–50.

133. Kilkovský B, Jegla Z. Preliminary design and analysis of regenerative heat exchanger. Chem Eng Trans. 2016; 52:655–60.

134. Yilmaz T, Büyükalaca O. Design of regenerative heat exchangers. Heat Transfer Engineering. 2003;24(4):32–8.

135. Shah RK, Sekuli DP. Selection of Heat Exchangers and Their Components. Fundamentals of Heat Exchanger Design. 2007. 673–734 p.

136. https://electricalworkbook.com/regenerator/.

137. https://electricalworkbook.com/regenerator/.

138. Wu J, Sun J, Liang L, Zha Y. Determination of weights for ultimate cross efficiency using Shannon entropy. Expert Syst Appl. 2011;38(5):5162–5.

139. Howedi, Aadel & Lotfi, Ahmad & Pourabdollah A. An Entropy-Based Approach for Anomaly Detection in Activities of Daily Living in the Presence of a Visitor. Entropy. 22(10.3390/e22080845):845.

140. Cengel, Yunus A.; BOLES, Michael A.; KANOĞLU, Mehmet. Thermodynamics: an engineering approach. New York: McGraw-hill, 2011.

141. BEJAN, Adrian. Advanced engineering thermodynamics. 1988..

142. Hesselgreaves JE. Compact Heat Exchangers: Selection, Design and Operation. Elsevier Science & Technology Books. 2001;83–123.

143. BOX, George EP; DRAPER, Norman R. Response surfaces, mixtures, and ridge analyses. John Wiley & Sons, 2007.

144. BAŞ, Cem. Cevap yüzeyi tasarımları ve sinir ağları yaklaşımı. 2010. PhD Thesis. University of Ankara.

145. CORNELL, John A. Experiments with mixtures: designs, models, and the analysis of mixture data. John Wiley & Sons, 2011.

146. Khuri, A.I., & Cornell, J.A., (1996). Response surfaces: Designs and analyses, second edition, Dekker, New York.

147. Aydar AY, Bağdatlıoğlu N, Köseoğlu O. Effect of ultrasound on olive oil extraction and optimization of ultrasound-assisted extraction of extra virgin olive oil by response surface methodology (RSM) ; Efecto del ultrasonido en la extracción de aceite de oliva y optimización de la extracción as. Grasas Aceites. 2017;68(189):17–3495.

148. Boyaci IH. A new approach for determination of enzyme kinetic constants using response surface methodology. Biochem Eng J. 2005;25(1):55–62.

149. Liu SK& H. Heat Exchangers: Selection, Rating and Thermal Design CRC Press. 2005. ISBN 0-8493-0902-6.

150. Ghozatloo A, Rashidi A, Shariaty-Niassar M. Convective heat transfer enhancement of graphene nanofluids in shell and tube heat exchanger. Experimental Thermal and Fluid Science. 2014 Feb; 53:136–41.

151. Technology. ST. Shell & Tube Heat Exchangers | UK Heat Exchanger Manufacturers.

152. Das, S. K., Choi, S. U. & P. H. E. Heat transfer in nanofluids—a review. Heat transfer engineering, 27(10):3-19..

153. A.K. Tiwari, P. Ghosh JS. Particles concentration levels of various nanofluids in plate heat exchanger for best performance, Int J Heat Mass Transf. 89:1110–1118.

154. Sarafraz M.M., F.Hormozi VN. Thermal performance of acounter-current double pipe heat exchanger working with COOH-CNT/water nanofluids, Exp Therm Fluid Sci. 78:41–49.

155. Bahiraei M, Rahmani R, Yaghoobi A, Khodabandeh E, Mashayekhi R, Amani M. Recent research contributions concerning use of nanofluids in heat exchangers: A critical review. Appl Therm Eng. 2018;133(January):137–59.

156. Çengel, Yunus A and AJGhajar. Heat and Mass Transfer: Fundamentals & Applications. New York: McGraw-Hill, 2011;

157. Wang J. Theory of flow distribution in manifolds. Chemical Engineering Journal. 2011;168(3):1331–45.

158. Wang J. Pressure drop and flow distribution in parallel-channel configurations of fuel cells: U-type arrangement. Int J Hydrogen Energy. 2008;33(21):6339–50.

159. Hewitt, Geoff F. and SJPugh. "Approximate design and costing methods for heat exchangers." Heat transfer engineering. 2007;28.2 :76–86.

160. Zhu D, Li X WN et al. Dispersion behavior and thermal conductivity characteristics of Al2O3–H2O nanofluids. Curr Appl Phys. 2009;131–139.

161. Ali, A.R.I., Salam BA. review on nanofluid: preparation, stability, thermophysical properties, heat transfer characteristics and application. SN Appl Sci. 2020;(2):1636.

162. Hamilton R.L., Crosser O.K.. Thermal conductivity of heterogeneous twocomponent systems, Industrial & Engineering Chemistry Fundamentals 1. 1962; 3:187–191.

163. F.J. Wasp. Solid–Liquid Slurry Pipeline Transportation, Trans Tech, Berlin. 1977.

164. H.C. Brinkman. The viscosity of concentrated suspensions and solution, Journal of Chemical Physics. 20:571–581.

165. X. Wang, X. Xu, S.U.S. Choi. Thermal conductivity of nanoparticles–fluid mixture, Journal of Thermophysics Heat Transfer. 13 (4):474–480.

166. G.K. Batchelor. The effect of Brownian motion on the bulk stress in a suspension of spherical particles, J Fluid Mech. 83 (1):97–117.

167. B.C. Pak, Y.I. Cho. Hydrodynamic and heat transfer study of dispersed fluids with

submicron metallic oxide particles, Experimental Heat Transfer. 11:151–170.

168. Esmaeili Sany a R, Saidi MH, Neyestani J. Experimental Prediction of Nusselt Number and Coolant Heat Transfer Coefficient in Compact Heat Exchanger Performed with ε-NTU Method. The Journal of Engine Research. 2010; 18:62–70.

169. Western Michigan University. 5.1 Shell-and-Tube Heat Exchangers. 1999;1–17.

170. Western Michigan University. 5.1 Shell-and-Tube Heat Exchangers. 1999;1–17.

171. Lu I, Weber NA, Bansal P, Fisher DE. Applying the effectiveness-NTU method to elemental heat exchanger models. ASHRAE Trans. 2007;113 PART 1(1):504–13.

172. Guo ZY, Liu XB, Tao WQ, Shah RK. Effectiveness-thermal resistance method for heat exchanger design and analysis. Int J Heat Mass Transf. 2010;53(13–14):2877–84.

173. Ogulata RT, Doba F. Experiments and entropy generation minimization analysis of a crossflow heat exchanger. Int J Heat Mass Transf. 1998;41(2):373–81.

174. Sahiti N, Krasniqi F, Fejzullahu X, Bunjaku J, Muriqi A. Entropy generation minimization of a double-pipe pin fin heat exchanger. Appl Therm Eng. 2008;28(17–18):2337–44.

175. Javadi FS, Sadeghipour S, Saidur R, BoroumandJazi G, Rahmati B, Elias MM, et al. The effects of nanofluid on thermophysical properties and heat transfer characteristics of a plate heat exchanger. International Communications in Heat and Mass Transfer. 2013; 44:58–63.

176. Elias MM, Miqdad M, Mahbubul IM, Saidur R, Kamalisarvestani M, Sohel MR, et al. Effect of nanoparticle shape on the heat transfer and thermodynamic performance of a shell and tube heat exchanger. International Communications in Heat and Mass Transfer. 2013; 44:93–9.

177. Zhou, J., Hatami, M., Song, D., Jing D. Design of microchannel heat sink with wavy channel and its time-efficient optimization with combined RSM and FVM methods. Int J Heat Mass Transf. 2016; 103 (https://doi.org/10.1016/j. ijheatmasstransfer.2016.07.100):715–724.